TECHNICAL REPORT 463-10

HYDROFOIL CRAFT DYNAMICS IN A REALISTIC SEA INCLUDING AUTOMATIC CONTROL

By

M. Martin

November 1967

HYDRONAUTICS, Incorporated

TECHNICAL REPORT 463-10

HYDROFOIL CRAFT DYNAMICS IN A REALISTIC SEA INCLUDING AUTOMATIC CONTROL

By

M. Martin

November 1967

Prepared for

Naval Ship Systems Command
Department of the Navy
Under
Contract Numbers
NObs-90224 and N00014-67-C-0417
SS600-000, Task 1701

TABLE OF CONTENTS

LIST OF FIGURES

I. INTRODUCTION

Preliminary studies of the dynamics of a hydrofoil boat are usually carried out using linear equations such as those described in Reference 1, in which the coefficients are based on existing experimental data and estimates. Such equations are usually sufficiently accurate for the initial studies but generally prove to be inadequate when more detailed information becomes available and when more accurate simulation is required. Important non-linearities must be included such as the effect of large depth changes on the wetted area of surface piercing hydrofoils and struts as well as on the hydrodynamic coefficients, of all submerged surfaces, ventilation effects, stall effects, interference effects at foil to foil and foil to strut junctures, and irregular effects at the point where the foils pierce the free water surface. Except for relatively simple configurations for which there already is a fair amount of data and theory, it is only feasible to use data obtained from a model of the complete foil - strut configuration to achieve a realistic simulation.

As a hydrofoil craft moves through the water in the foil-borne mode, the foils and struts experience changes in submergence, speed and angle of attack because of the boat motions and the variations in height and orbital motions of the waves. Because of the different location on the boat of the various foils and struts these changes will be different, in general, at each of these locations. It therefore becomes necessary to obtain the submergence, wetted area, speed and angle of attack at each foil

and strut separately before determining the hydrodynamic force acting on it. For very large foils the foil is considered to be made up of two or three segments or panels of convenient size in order to account for the differences in flow conditions, submergence and moment arm that may occur at different parts of the same foil.

II. EQUATIONS OF MOTION

The equations for the dynamics of the craft are written in terms of the conventional x,y,z right handed system of axes fixed in the body, with origin at the center of gravity (See Figure 1). The xz plane is taken in the vertical plane of symmetry with the z axis positive downward. These axes are convenient because the moments and products of inertia defined relative to them remain constant provided the mass of the boat does not change significantly. Furthermore velocities and accelerations determined with respect to these axes are the same as those measured by instruments mounted in the craft.

The equations for the three force and three moment components are (1):

$$m(\dot{u} + qw - rv) = X - mg \sin \theta \qquad [1a]$$

$$m(\dot{v} + ru - pw) = Y + mg \cos \theta \sin \phi \qquad [1b]$$

$$m(\dot{w} + pv - qu) = Z + mg \cos \theta \cos \phi \qquad [1c]$$

$$I_{xx}\dot{p} + (I_{zz} - I_{yy})qr - I_{zx}(\dot{r} + pq) = K \qquad [2a]$$

$$I_{yy}\dot{q} + (I_{xx} - I_{zz})rp + I_{zx}(p^2 - r^2) = M \qquad [2b]$$

$$I_{zz}\dot{r} + (I_{yy} - I_{xx})pq + I_{zx}(qr - \dot{p}) = N \qquad [2c]$$

where the standard SNAME nomenclature is used (2) and the usual relationships between fixed and body axes apply. These are defined below for convenience.

We describe a right handed set of coordinates fixed in space by x_o, y_o, z_o where z_o is positive downward and parallel to the gravity axis. We also define a set of Euler angles ψ, θ and ϕ which describe the angular orientation of the x,y,z axes with respect to the x_o, y_o, z_o axes (see Figure 1). If x and x_o are initially parallel then ψ is the angular rotation about the z_o axis (the angle between the y_1 and y_o axes), θ is the angular rotation about the y_1-axis (the angle between the z_2 and z_o axes) and ϕ is the angular rotation about the x axis, where the rotations are performed in the order stated. Thus, given a vector in earth axes, we can determine the components of this vector in body axes by means of these rotations carried out in the order given. The product of these three rotations result in a rotation matrix. The product of this matrix with a vector whose components are given in fixed axes yields the body axes components. Hence (1),

$$\begin{bmatrix} \cos\theta\cos\psi & \cos\theta\sin\psi & -\sin\theta \\ \cos\psi\sin\theta\sin\phi - \sin\psi\cos\phi & \cos\psi\cos\phi + \sin\psi\sin\theta\sin\phi & \cos\theta\sin\phi \\ \cos\psi\sin\theta\cos\phi + \sin\psi\sin\phi & \sin\theta\cos\phi\sin\psi - \sin\phi\cos\psi & \cos\theta\cos\phi \end{bmatrix} \begin{bmatrix} V_{xo} \\ V_{yo} \\ V_{zo} \end{bmatrix} = \begin{bmatrix} V_x \\ V_y \\ V_z \end{bmatrix} \quad [3]$$

where (V_{xo}, V_{yo}, V_{zo}) are the components of a vector V in fixed axes and (V_x, V_y, V_z) are its components in body axes. Thus the three components of the gravity vector in body axes shown on the right hand side of Equation [1] is obtained from Equation [3] by replacing (V_{xo}, V_{yo}, V_{zo}) by (0, 0, mg).

Since the rotational matrix is an orthogonal one the matrix giving the vector components in fixed axes of any vector expressed in body axes is simply the transpose of the square matrix given in Equation [3]. This is obtained by interchanging rows and columns. Thus,

$$\begin{bmatrix} \cos\theta\cos\psi & \cos\psi\sin\theta\sin\phi - \sin\psi\cos\phi & \cos\psi\sin\theta\cos\phi + \sin\psi\sin\phi \\ \cos\theta\sin\psi & \cos\psi\cos\phi + \sin\psi\sin\theta\sin\phi & \sin\theta\cos\phi\sin\psi - \sin\phi\cos\psi \\ -\sin\theta & \cos\theta\sin\phi & \cos\theta\cos\phi \end{bmatrix} \begin{bmatrix} V_x \\ V_y \\ V_z \end{bmatrix} = \begin{bmatrix} V_{xo} \\ V_{yo} \\ V_{zo} \end{bmatrix} \quad [4]$$

The equations giving the velocity of the c.g. of the boat in fixed coordinates is obtained by replacing (V_x, V_y, V_z) in the above equation by (u, v, w) giving (1)

$$\dot{x}_o = u \cos\theta \cos\psi + v (\sin\theta \sin\phi \cos\psi - \cos\phi \sin\psi) + w (\sin\phi \sin\psi + \sin\theta \cos\phi \cos\psi) \quad [5a]$$

$$\dot{y}_o = u \cos\theta \sin\psi + v (\sin\theta \sin\phi \sin\psi + \cos\phi \cos\psi) + w (-\sin\phi \cos\psi + \sin\theta \cos\phi \sin\psi) \quad [5b]$$

$$\dot{z}_o = -u \sin\theta + v \cos\theta \sin\phi + w \cos\phi \cos\theta \quad [5c]$$

The position of the craft c.g. is obtained from

$$x_o = \int \dot{x}_o dt \quad ; \quad y_o = \int \dot{y}_o dt \quad ; \quad z_o = \int \dot{z}_o dt \quad [6]$$

It is also of interest to determine the angular orientation of the craft. Since it will be recalled that the Euler angles ψ, θ and ϕ are not measured about orthogonal axes Equation [4] cannot be used. However the relationships between the Euler angle rates and the angular rates in body axes are readily derivable (1) and are given by the following equations:

$$p = \dot{\phi} - \dot{\psi} \sin \theta \qquad [7a]$$

$$q = \dot{\theta} \cos \phi + \dot{\psi} \cos \theta \sin \phi \qquad [7b]$$

$$r = \dot{\psi} \cos \theta \cos \phi - \dot{\theta} \sin \phi \qquad [7c]$$

$$\dot{\theta} = q \cos \phi - r \sin \phi \qquad [8a]$$

$$\dot{\phi} = p + q \sin \phi \tan \theta + r \cos \phi \tan \theta \qquad [8b]$$

$$\dot{\psi} = (q \sin \phi + r \cos \phi) \sec \theta \qquad [8c]$$

and the Euler angles are

$$\theta = \int \dot{\theta} \, dt \; ; \quad \phi = \int \dot{\phi} \, dt \; ; \; \psi = \int \dot{\psi} \, dt \qquad [9]$$

Equations [1], [2] and [5-9] are completely general and sufficient to define the motions of the craft, treated as a rigid body, in response to forces and moments of any magnitude. Hydrofoil motions however are relatively limited. According to Reference 3 malfunction studies have indicated that roll angles of 15 degrees and larger may occur during abnormal situations on some hydrofoil craft. For this reason it may be desirable to retain trigonometric functions of the roll angle. However, from

studies to date craft pitch angles are not expected to reach as high as 10 degrees. In normal operation the pitch angle is usually less than 3 degrees. Consequently, it is justified to use the small angle approximation of

$$\sin\theta = \theta \quad ; \quad \cos\theta = 1 \qquad [10]$$

in the above equations. Although an insufficient number of configurations have been studied to justify a general statement concerning the importance of the I_{zx} term in Equation [2] it appears to be typically less than 10 percent of I_{xx} and less than 4 percent of I_{yy} and I_{zz}. Thus, when multiplied by terms of the magnitude of $(\dot{r} + pq)$, (p^2-r^2), $(qr - \dot{p})$ the effect of I_{zx} may be negligible in specific cases. The importance of the gyroscopic term $(I_{zz} - I_{yy})qr$ in Equation [2a] is best determined from a comparison of dynamic response calculations with and without this term. If the difference is negligible the term may be deleted in subsequent computations. The same tests are also useful when applied to the rv, pw and pv terms in Equation [1].

III. CALCULATION OF HYDRODYNAMIC FORCES

A. Resolution of Foil Forces Into Boat Axes

As mentioned earlier various parts of the strut and foil system experience different speeds, submergences and angles of attack as it is tossed about in the waves. It is therefore necessary to determine the force and moment contribution from each foil

and strut separately. Since there is a large variety of configurations it is desirable to adopt a nomenclature for identifying the struts and foils and their locations, which can have general applicability. Subscripts in the form of letters has been found convenient in the past (3), (4), (5). Table 1, which gives the symbols that define the various force components and their locations for the foil system shown in Figure 2, is an example of this technique, and will be used in the subsequent paragraphs to illustrate its application. The main strut-foil system shown is considered to be made up of two submerged foil segments, two anhedral and two dihedral surface piercing foil segments, and two struts. The symbols for the starboard foil segment is (sf), the port foil segment (pf), etc. As shown in Table 1, these subscripts are used in conjunction with the X, Y, Z force components and x, y, z components of the position vector at which the force acts, both given in the body axes. Although the use of numerical subscripts is also satisfactory it is not as convenient for identification of the struts and foils. In the following sections the subscript f will be used to represent an unspecified foil segment or strut.

Force data on foils is usually obtained in terms of three orthogonal vector components, viz, drag (D_f), lift (L_f) and cross force (C_f). The last of these (C_f) usually makes a relatively small contribution to the overall force components of typical hydrofoil boats and is often neglected. Since these force components are functions of angle of attack, angle of sideslip, submergence, speed and flap angle it is therefore necessary to first

determine the values of each of these variables in the foil axis system. Figure 3 defines the angle of attack α_f, the angle of sideslip β_f and the velocity axes for an individual foil (or panel), with respect to the foil axes, represented by the unit orthogonal vectors $\vec{i}_f$, $\vec{j}_f$, $\vec{k}_f$. $\vec{V}_f$ is the local velocity vector of the origin of the foil axes relative to the fluid and is coincident with the unit vector $\vec{i}_v$. The hydrodynamic force on the foil is represented by

$$\vec{F}_f = - D_f\vec{i}_v + C_f\vec{j}_v - L_f\vec{k}_v \qquad [11]$$

where unit vectors $\vec{i}_v$, $\vec{j}_v$, $\vec{k}_v$ are parallel to the local velocity axes referred to the point O on the foil. The force $\vec{F}_f$ is resolved into the X, Y, Z force components in the boat body axes (See also Figure 4) x, y, z (parallel to the unit vectors $\vec{i}$, $\vec{j}$, $\vec{k}$) by a transformation via the intermediate set of foil axes $\vec{i}_f$, $\vec{j}_f$, $\vec{k}_f$ as follows. Any vector $\vec{v}$ in the velocity axes may be expressed in terms of the foil axes by the following transformation (5)

$$\begin{vmatrix} \vec{v}\cdot\vec{i}_f \\ \vec{v}\cdot\vec{j}_f \\ \vec{v}\cdot\vec{k}_f \end{vmatrix} = \begin{vmatrix} \cos\alpha_f & 0 & -\sin\alpha_f \\ 0 & 1 & 0 \\ \sin\alpha_f & 0 & \cos\alpha_f \end{vmatrix} \begin{vmatrix} \cos\beta_f & -\sin\beta_f & 0 \\ \sin\beta_f & \cos\beta_f & 0 \\ 0 & 0 & 1 \end{vmatrix} \begin{vmatrix} \vec{v}\cdot\vec{i}_v \\ \vec{v}\cdot\vec{j}_v \\ \vec{v}\cdot\vec{k}_v \end{vmatrix} \qquad [12]$$

In Figure 4 the foil axes are shown relative to the boat body axes, x, y, z. The dihedral angle Γ is defined as follows. The foil axes are imagined to be initially parallel to the body axes $(\vec{i}, \vec{j}, \vec{k})$. Then rotate the foil axes about the $\vec{i}$ axis an angle Γ so that the foil axes have the directions $\vec{i}_f$, $\vec{j}_f$, $\vec{k}_f$. The usual sign convention of a right handed system holds. Thus as shown in the figure the starboard foil dihedral angle has a negative sign and the port foil dihedral angle a positive sign when the dihedral is positive in the conventional sense. A strut may be considered to be a foil of symmetrical section with a dihedral angle of either plus or minus 90° provided the axes conventions defined by Figures 3 and 4 are adhered to. With the dihedral defined in this manner, a vector $\vec{v}$ in the foil axes may be written in terms of the body axes as follows

$$\begin{vmatrix} \vec{v} \cdot \vec{i} \\ \vec{v} \cdot \vec{j} \\ \vec{v} \cdot \vec{k} \end{vmatrix} = \begin{vmatrix} 1 & 0 & 0 \\ 0 & \cos \Gamma_f & -\sin \Gamma_f \\ 0 & \sin \Gamma_f & \cos \Gamma_f \end{vmatrix} \begin{vmatrix} \vec{v} \cdot \vec{i}_f \\ \vec{v} \cdot \vec{j}_f \\ \vec{v} \cdot \vec{k}_f \end{vmatrix} \qquad [13]$$

By combining Equations [12] and [13] we obtain the matrix which transforms a vector in the velocity axes into one in the body axes. Thus the X, Y, Z components of $\vec{F}_f$ of Equation [11] are obtained by means of the following transformation.

$$\begin{vmatrix} X_f \\ Y_f \\ Z_f \end{vmatrix} = \begin{vmatrix} \cos\beta_f \cos\alpha_f & -\sin\beta_f \cos\alpha_f & -\sin\alpha_f \\ \sin\beta_f\cos\Gamma_f & \cos\beta_f\cos\Gamma_f & -\cos\alpha_f\sin\Gamma_f \\ -\cos\beta_f\sin\alpha_f\sin\Gamma_f & +\sin\beta_f\sin\alpha_f\sin\Gamma_f & \\ \sin\beta_f\sin\Gamma_f & \cos\beta_f\sin\Gamma_f & \cos\alpha_f\cos\Gamma_f \\ +\cos\beta_f\sin\alpha_f\cos\Gamma_f & -\sin\beta_f\sin\alpha_f\cos\Gamma_f & \end{vmatrix} \begin{vmatrix} -D_f \\ C_f \\ -L_f \end{vmatrix} \quad [14]$$

B. Determination of Foil Angle of Attack and Sideslip Angle

The determination of α_f and β_f is given below for a specific foil segment. Corresponding relationships for any other foil segment or strut are obtained by substituting the appropriate subscript. The angle of attack on, say the starboard, dihedral foil segment, α_{sd}, and the sideslip angle β_{sd}, are defined by Figure 3 in terms of the components of the relative velocity vector $V_{sd}\vec{u}_v$ resolved along the foil segment axes. These are obtained as follows. If x_{sd}, y_{sd} and z_{sd} are the coordinates of the origin O_{sd} of the foil axis system relative to the C.G. (taken as the point where the foil force is considered to act) then the three components of the velocity of O_{sd} relative to the water resolved along the body axes are

$$\begin{aligned} u_{sd} &= u + qz_{sd} - ry_{sd} - u'_{sd} - u''_{sd} \\ v_{sd} &= v + rx_{sd} - pz_{sd} - v'_{sd} - v''_{sd} \\ w_{sd} &= w + py_{sd} - qx_{sd} - w'_{sd} - w''_{sd} \end{aligned} \quad [15]$$

where

u_{sd}', v_{sd}', w_{sd}' are the x, y, z components in body axes of the orbital velocity due to waves at the point x_{sd}, y_{sd}, z_{sd} (See Section IV),

u_{sd}'', v_{sd}'', w_{sd}'' are the x, y, z components in body axes of the wake effects resulting from side wash, downwash, separation etc. (applies* mainly to aft foils and struts).

These velocity components are then expressed in terms of the foil axes by means of the inverse transformation of Equation [13]. Thus,

$$\begin{vmatrix} u_{sdf} \\ v_{sdf} \\ w_{sdf} \end{vmatrix} = \begin{vmatrix} 1 & 0 & 0 \\ 0 & \cos \Gamma_{sd} & \sin \Gamma_{sd} \\ 0 & -\sin \Gamma_{sd} & \cos \Gamma_{sd} \end{vmatrix} \begin{vmatrix} u_{sd} \\ v_{sd} \\ w_{sd} \end{vmatrix} \qquad [16]$$

---

* Methods of estimating these effects are described in Reference 5. Studies on specific configurations (6), (7), (8) have shown that downwash effects had very little effect on the motions.

where u_{sdf}, v_{sdf}, w_{sdf} are the velocity components of O_{sd} relative to the water resolved along the foil axes. The angle of attack is defined by

$$\alpha_{sd} = (\alpha_o)_{sd} + \tan^{-1} \frac{w_{sdf}}{u_{sd}} \qquad [17a]$$

and the side slip angle by

$$\beta_{sd} = \sin^{-1} \frac{v_{sdf}}{[u_{sd}^2 + v_{sd}^2 + w_{sd}^2]^{\frac{1}{2}}} \qquad [18a]$$

where $(\alpha_o)_{sd}$ is the effective fixed incidence angle, if any, on the foil. At high craft speeds the angles of attack and sideslip are rarely greater than 10 degrees. Furthermore, except for relatively slow speeds the denominators in Equations [17] and [18] can be approximated quite well by u so that for these cases

$$\alpha_{sd} = (\alpha_o)_{sd} + \frac{w_{sdf}}{u} \qquad [17b]$$

$$\beta_{sd} = \frac{v_{sdf}}{u} \qquad [18b]$$

It might be noted that for a vertical strut, say the rear strut, we may take* $\Gamma_{rs} = \pm 90^{o}$. Equation [16] then gives for the rear strut

$$u_{rsf} = u_{rs}$$

$$v_{rsf} = \begin{cases} w_{rs} & \text{for } \Gamma_{rs} = +90 \\ -w_{rs} & \text{for } \Gamma_{rs} = -90 \end{cases}$$

$$w_{rsf} = \begin{cases} -v_{rs} & \text{for } \Gamma_{rs} = +90 \\ v_{rs} & \text{for } \Gamma_{rs} = -90 \end{cases}$$

According to Equations [17] and [18] with $\alpha_{o} = 0$, the sign of α_{rs} and β_{rs} depends on the sign selected for Γ. Since, as implied earlier, the foil (or strut) axes for $\Gamma = +90^{o}$ is turned 180^{o} about the x-axis from that for $\Gamma = -90^{o}$ the sign for a given lift** (L_{rs}) and cross force (C_{rs}) is opposite for the two cases. However, this does not affect the sign of the X_{rs}, Y_{rs}, Z_{rs} components in the boat body axes, as determined from Equation [14], since a change in sign of C_{rs} and L_{rs} is accompanied by a change in sign of α_{rs}, β_{rs} and Γ_{rs}.

---

* One advantage in choosing $\Gamma_{rs} = +90^{o}$ is that the rudder rotation is positive in the same sense as is the elevator rotation for a $\Gamma = 0$ foil.

** As implied by Equation [14] the lift is defined in the velocity foil axis systems. Thus the lift on a horizontal foil is up and on a vertical foil (or strut) sideways.

C. Submergence of a Completely Submerged Foil Panel

The foil submergence depends on the instantaneous position and attitude of the craft and the wave height at the point of interest. As an example we select the starboard foil panel designated with the subscript sf shown in Figure 2. The instantaneous submergence of this panel is given by

$$h_{sf} = d_{sf} + z_{oc} - h_c - \eta_{sf} \qquad [19]$$

where

h_{sf} is the submergence of the middle of the starboard foil in fixed axes below the instantaneous water surface,

d_{sf} is the vertical distance, in fixed axes, of the C.G. to the middle of the starboard foil,

z_{oc} is the vertical displacement of the C.G.,

h_c is the vertical distance of the C.G. from the undisturbed water surface under reference flight conditions, and

η_{sf} is the wave elevation from the undisturbed water surface directly above the middle of the starboard foil, positive down (see Section IV).

It must be remembered that all positive distances are measured downward from the reference points. In Equation [19] the term z_{oc} is obtained from the last of Equations [6] and the term d_{sf} is obtained by the use of the body to earth transformation matrix

of Equation [4] where the position vector of point sf (x_{sf}, y_{sf}, z_{sf}) replaces (V_x, V_y, V_z) and d_{sf} replaces V_{zo}. Thus

$$d_{sf} = - x_{sf} \sin \theta + y_{sf} \cos \theta \sin \phi + z_{sf} \cos \theta \cos \phi \qquad [20a]$$

In nearly all cases θ is small so that

$$d_{sf} = - x_{sf} \theta + y_{sf} \sin \phi + z_{sf} \cos \phi \qquad [20b]$$

The expression for the wave elevation η_{sf} is given in Section IV. In a similar manner, the submergence of any other point may be determined. In the above example it is assumed that when h_{sf} is negative the entire starboard foil panel is out of the water and the submerged area is zero; i.e.,

$$S_{sf} = \begin{cases} (S_{sf})_o & \text{for } h_{sf} > 0 \\ 0 & \text{for } h_{sf} < 0 \end{cases} \qquad [21]$$

where

S_{sf} is the wetted planform area at any instant,

$(S_{sf})_o$ is the wetted planform area in level equilibrium flight.

Obviously more complicated relationships would be required if it were desired to specify the wetted area during partial submergence. Although this refinement is usually not needed when dealing with segments of completely submerged foils it is very important for the case of surface piercing segments such as struts and foils with dihedral or anhedral. This is discussed in the next section.

D. Area of Surface Piercing Panel or Strut

The foil wetted planform area is a variable only when the foils and struts pierce the free surface. Since the spanwise distribution of chord length is known it is only necessary to find the change in wetted length of the surface piercing foil, strut, or panel from its reference value. This computation is illustrated in the following example for the port panel with dihedral as shown in Figure 5a before and 5b after roll angle $+\phi$, for the case of θ, z_{oc}, and wave height equal to zero. The wetted length of the port dihedral panel is imagined extended until it intersects the plane of symmetry of the boat. The reference wetted length of this extended panel is

$$(\ell_r)_{pd} = \frac{(z_e)_{pd} - h_c}{|\sin \Gamma|}$$

where $(z_e)_{pd}$ is the distance between the boat CG and the point of intersection of the extended dihedral panel with the xz plane. The final wetted length of the extended panel after a roll angle ϕ^* is easily seen to be

---

* It is assumed here that $|\Gamma| > |\phi|$.

$$(\ell_f)_{pd} = \pm \frac{(z_e)_{pd} \cos \phi - h_c}{\sin (\Gamma_{pd} + \phi)} \quad \begin{cases} + \text{ for } \Gamma_{pd} > 0 \\ - \text{ for } \Gamma_{pd} < 0 \end{cases}$$

Therefore the change in wetted length due to roll angle only is

$$(\Delta \ell_{pd})_\phi = (\ell_f)_{pd} - (\ell_r)_{pd} = \frac{(z_e)_{pd} \cos \phi - h_c}{\sin (\Gamma_{pd} + \phi)} - \frac{(z_e)_{pd} - h_c}{\sin \Gamma_{pd}} \text{ for } \Gamma_{pd} > 0 \qquad [22a]$$

For the starboard panel, where Γ is negative, the same expression holds except that a minus sign precedes it; i.e.,

$$(\Delta \ell_{sd})_\phi = - \frac{(z_e)_{sd} \cos \phi - h_c}{\sin (\Gamma_{sd} + \phi)} + \frac{(z_e)_{sd} - h_c}{\sin \Gamma_{sd}} \text{ for } \Gamma_{sd} < 0 \qquad [22b]$$

The effects of θ, z_{oc} and wave height are additive so that the total change in wetted length of the extended panel is given by

$$(\Delta \ell_{pd}) = \frac{(z_e)_{pd} \cos \phi - h_c - x_{pd}\theta + z_{oc} - \eta_{pd}}{\sin (\Gamma_{pd} + \phi)} - \frac{(z_e)_{pd} - h_c}{\sin \Gamma_{pd}} \text{ for } \Gamma_{pd} > 0$$

[23a]

$$(\Delta\ell_{sd}) = -\frac{(z_e)_{sd}\cos\phi - h_c - x_{sd}\theta + z_{oc} - \eta_{sd}}{\sin(\Gamma_{sd} + \phi)} + \frac{(z_e)_{sd} - h_c}{\sin\Gamma_{sd}} \quad \text{for } \Gamma_{sd} < 0 \qquad [23b]$$

where for vertical struts $\Gamma = \pm 90^{\circ}$. In the above expressions η_{pd} and η_{sd} are the wave elevations at the point of intersection with the free surface of the pd and sd panels respectively. The use of the reference value of this point at level flight should be a sufficiently good approximation. If the actual length of the foil or strut segment below the free surface at reference flight conditions is $(\ell_{pd})_b$ and the length above the reference water surface is $(\ell_{pd})_a$ (see Figure 5a), then the wetted area is given by

$$S_{pd} = (S_{pd})_o + \int_o^{s_{pd}} c\, ds \qquad [24]$$

where

$$s_{pd} = \begin{cases} -(\ell_{pd})_b & \text{for} \quad (\Delta\ell_{pd}) < -(\ell_{pd})_b \\ \Delta\ell_{pd} & \text{for} \quad (\ell_{pd})_a > (\Delta\ell_{pd}) > -(\ell_{pd})_b \\ (\ell_{pd})_a & \text{for} \quad (\Delta\ell_{pd}) > (\ell_{pd})_a \end{cases}$$

$$(S_{pd})_o = -\int_o^{-(\ell_{pd})_b} c\, ds$$ is the wetted planform area at reference flight conditions, and

c is the panel chord length which may be a function of spanwise position s_{pd}.

Since struts and anhedral surface piercing foils almost always intersect the boat hull the condition $(\Delta \ell_{ps}) > (\ell_{ps})_a$, for example, implies hull wetting. The degree of hull wetting can be determined from the magnitude of $(\Delta \ell_{ps})-(\ell_{ps})_a$.

The above equations are used when $|\phi| < |\Gamma|$. When $|\phi| \geq |\Gamma|$ then it usually may be assumed that the change in area is the same as when $|\phi| = |\Gamma|$; i.e. one of the dihedral foil segments is either completely submerged or completely out of the water. When $\phi \geq \Gamma$ the starboard dihedral foil segment would be thus affected while the above equations would still apply to the port dihedral segment. When $\phi \leq -\Gamma$ the reverse would apply. The condition for submergence for the affected foil segment may be determined in the same manner as for a completely submerged foil (see Equations [19-21]). The position vector to the dihedral foil segment in question may be taken at its center of force at reference flight conditions as a first approximation.

E. Center of Force and Submergence of Surface Piercing Panels and Struts

Since different points on surface piercing panels and struts are at different depths the point of application of the water forces will vary with the degree of submergence. Strictly speaking this also depends on the panel or strut section shape and on the flow interference effects at the foil and strut intersection (3)(5). However, according to these references, detailed

calculations on typical vertical struts indicate that a value of 0.6 of the submergence of the lower end below the free surface is common. In the absence of experimental data this is probably a reasonably good approximation for most surface piercing panels also (5). Thus if for example $(x_{ps}', y_{ps}', z_{ps}')^*$ represents the position vector, in body axes, of the bottom of the port strut then the position vector (x_{pd}, y_{pd}, z_{pd}) at which the water force is applied to the pd panel is defined by (see Figure 2)

$$\left.\begin{aligned} x_{pd} &= x_{ps}' \\ y_{pd} &= y_{ps}' - [(\ell_{pd})_b + s_{pd}]\, 0.4 \cos \Gamma_{pd} \\ z_{pd} &= z_{ps}' - [(\ell_{pd})_b + s_{pd}]\, 0.4 \sin \Gamma_{pd} \end{aligned}\right\} \quad \text{for } \Gamma_{pd} > 0 \qquad [25a]$$

For the sd panel we have

$$\left.\begin{aligned} x_{sd} &= x_{ss}' \\ y_{sd} &= y_{ss}' + [(\ell_{sd})_b + s_{sd}]\, 0.4 \cos \Gamma_{sd} \\ z_{sd} &= z_{ss}' + [(\ell_{sd})_b + s_{sd}]\, 0.4 \sin \Gamma_{sd} \end{aligned}\right\} \quad \text{for } \Gamma_{sd} < 0$$

---

* The prime is used here to differentiate from the unprimed quantity which gives the position vector of the center of force.

As noted earlier $\Gamma = \pm 90^{\circ}$ for vertical struts. In the above equations, due to symmetry, we have

$$(\ell_{pd})_b = (\ell_{sd})_b$$

$$(x_{ss}', y_{ss}', z_{ss}') = (x_{ps}', -y_{ps}', z_{ps}') \qquad [25c]$$

The factor 0.4 is based on the assumption that the center of panel force is located at 0.6 of the vertical projection of the panel wetted length below the free surface; e.g., for the port dihedral panel

$$h_{pd} = 0.6\,[(\ell_{pd})_b + s_{pd}] \sin(\Gamma_{pd} + \phi) \text{ since } \Gamma > 0 \qquad [26a]$$

and for the starboard dihedral panel

$$h_{sd} = -0.6\,[(\ell_{sd})_b + s_{sd}] \sin(\Gamma_{sd} + \phi) \text{ since } \Gamma < 0 \qquad [26b]$$

Equation [26] may be used as an approximate expression for the effective depth of submergence of a surface piercing hydrofoil segment. The use of data and analysis is recommended for more precise estimates of this quantity (see Reference 5).

F. Hydrodynamic Force Coefficients

As noted earlier, the hydrodynamic force on a strut or foil segment is generally obtained in terms of the lift, drag and cross force coefficients. The effect of the last of these is usually small and has generally been assumed to be negligible in mathematical simulations carried out in the past. These coefficients are usually non-dimensionalized with respect to foil speed and area. Thus

$$C_{Lf} = \frac{L}{\frac{1}{2}\rho U_f^2 S_f} \quad ; \quad C_{Df} = \frac{D_f}{\frac{1}{2}\rho U_f^2 S_f} \quad ; \quad C_{Cf} = \frac{C_f}{\frac{1}{2}\rho U_f^2 S_f} \qquad [27]$$

where

f identifies the foil panel or strut; e.g., f = sd or f = pd, etc.,

U_f^2 is the square of the foil velocity relative to the water. For the starboard dihedral panel for example this would be $u_{sd}^2 + v_{sd}^2 + w_{sd}^2$ as obtained from Equation [15],

S_f is the foil panel or strut area determined at any instant from Equation [24],

L_f is the lift force on foil panel or strut f,

D_f is the drag force on foil panel or strut f,

C_f is the cross force on foil panel or strut f, and

ρ is the mass density of water.

In most cases it will be satisfactory to approximate U_f by u, the x-component of the velocity of the craft C.G. However, in waves at low craft speeds the total relative velocity U_f should be used. The coefficients in Equation [27] are functions of angle of attack, angle of side slip, submergence, velocity, and flap angle.

Except for conditions when the relationships are linear it is not possible to derive analytical expressions for these coefficients (3),(5),(9). This is due to the difficulties in predicting the occurrence and cessation of cavitation and ventilation, the non-linear variation with the individual variables, free surface effects, downwash, strut-foil interference, finite discontinuities, elastic effects, unsteady flow, etc. It is therefore felt that model test data in conjunction with available full-scale data and theory are the most appropriate means for describing the dependence of C_L and C_D on the other variables at the present time. Hence the usual form of the data from these sources will be discussed.

1. Lift Coefficient - Although it is recognized that many foil designs, each with different hydrodynamic characteristics, are possible for hydrofoil craft, it will be assumed, for the sake of expediency, that the curves discussed here are more or less typical of a wide class of hydrofoils. Hydrofoils with different characteristics would be handled in an analogous manner. The principle point to be emphasized is that it is necessary to

use realistic representations of any non-linear phenomena that may exist.

We use as an example a foil of conventional section whose mathematical simulation is discussed in Reference 3b. The flow and corresponding portions of the typical lift coefficient curve are shown in Figure 6.* Three types of flow are depicted. This is not an all-inclusive representation because the several conditions which are possible in the mixed or transition region are not shown in the sketches. The C_L versus α characteristics is typical however. A detailed description of the conditions relating to the onset of cavitation and ventilation for various types of foils and struts is given in Reference 10.

The location of point "A" of Figure 6 indicates the value of C_L at zero angle of attack. From point "A" to point "B" the slope of the curve is usually constant and is the portion usually considered in a simplified linear analysis. At point "B" cavitation bubbles begin to form and the slope of the curve begins to change. The shape of the curve from "B" to "C" is not well defined; it is here assumed to be a straight line extension of the line "AB." At "C" complete flow separation occurs at the top surface of the foil and the lift abruptly decreases. It is common to refer to this event as the "lift break." From "D" to "E" and back to "F" the slope is essentially constant again and the foil is operating with the upper surface completely unwetted.

---

* Parts of the following discussion are essentially that given in Reference 3b.

The line "FG" indicates that re-wetting will occur as the angle of attack is decreased. However, the exact location of this line is difficult to define. Also, it should be recognized that the exact C_L for any α between α_1 and α_2 is indeterminate. The area enclosed by BCDFGB is thus an area of uncertainty. A similar sequence of events occurs as the angle of attack decreases below zero and returns.

In Figure 6, the abrupt lift changes are indicated as occurring at four sloping lines. For convenience in the following discussion, these lines will be identified as described below. Note that in the description the term "limit" is the limit of a trend and not an absolute boundary.

C_{L+IL} = Limit value of C_L for increasing values of positive C_L or "C_L positive, increasing; limit"

C_{L+DL} = C_L positive, decreasing; limit

C_{L-DL} = C_L negative, decreasing; limit

C_{L-IL} = C_L negative, increasing; limit

where

"increasing" refers to C_L moving from bottom to top any place along the ordinate, and

"decreasing" refers to C_L moving from top to bottom.

The positions of these four lines have been found to depend on angle of attack, α, craft velocity, U, and foil submergence, h. Further, the dependency can be expressed in the general case as:

$$C_{L\ limit} = [f_L(U) + K_L h] + K_\alpha \alpha \qquad [28]$$

which can be thought of as the slope-intercept equation of a straight line where the intercept with the ordinate occurs at $f_L(U) + K_L h$ and the slope is K_α. The form of $f_L(U)$ will be shown later.

Actuation of the trailing edge flaps, by the pilot or control system, for craft motion control results in further modification of the C_L - α representation. Figure 7a indicates how the lift curve shifts for positive (down) and negative (up) flap angles δ. The degree values on the curves are only meant to indicate relative changes. It is intended to show that for the lower values of δ, equal increments of δ give equal increases in C_L. (See Figure 7b). However, at some positive δ, flow will separate from the upper surface of the flap and the plot of C_L versus δ will take on a decreased slope. (Shown, for example, as occurring at 10 degrees in Figure 7b). A similar effect takes place for negative δ. There is also the possibility that very large flap deflections will cause the foil to unwet as C_L exceeds $C_{L\ limit}$. The contributions of the control deflection, δ, to the value of C_L are shown in Figure 7b in terms of an increment, ΔC_L. As shown, it is assumed that no hysteresis is associated solely with unwetting due to δ.

In addition to its effect on the position of the C_L-limit lines, submergence also affects $C_{L\alpha}$, the slope of the C_L curve. This can be shown as in Figure 8 where the ordinate has been normalized by dividing by the value of $C_{L\alpha}$ at infinite submergence. Note the difference between the effect for wetted flow and the effect for cavitated flow. Figure 9 is a similar curve for a strut or surface piercing foil but normalized to a finite reference depth h_r. The shape of this curve reflects the dominant effect of changing aspect ratio with changing depth on the effective lift curve slope (5).

The factors which contribute to C_L have been discussed but it remains to summarize the effects in some sort of useful form. From the discussion and figures to this point, it is possible to discern that:

(1) One set of properties applies if the flow is fully wetted,

(2) A second set of properties applies if the flow is fully cavitated, and

(3) Whether the fully wetted or cavitated properties apply at any instant depends on a set of "control" equations which define the conditions when cavitation occurs and ceases.

In effect, C_L must be continuously calculated for both the fully wetted and fully cavitated properties. The "control" equations then determine which C_L is to be used as a part of the total system equations at each instant.

The fully wetted C_L is calculated from:

$$C_{Lw} = [f_w(\alpha) + f_w(\delta)][f_w(h)] \qquad [29]$$

Values of the functions will be taken from graphs such as depicted in Figures 8a or 9 and 10a. The depth correction factor $f_w(h)$ can be readily obtained with respect to any reference depth with the aid of data such as that in Figure 8a.

The fully cavitated C_L is calculated from a similar equation:

$$C_{Lc} = [f_c(\alpha) + f_c(\delta)][f_c(h)] \qquad [30]$$

But the functions will, of course, be different as shown in Figures 8b and 10b. In Figure 10 note that the slope of $f_w(\alpha)$ is steeper than the slope of $f_c(\alpha)$.

There are four "control" equations of similar form:

$$C_{L+IL} = f_{L1}(U) + K_{L1}h + K_\alpha\alpha \qquad [31]$$

$$C_{L+DL} = f_{L2}(U) + K_{L2}h + K_\alpha\alpha \qquad [32]$$

$$C_{L-DL} = f_{L3}(U) + K_{L3}h + K_\alpha\alpha \qquad [33]$$

$$C_{L-IL} = f_{L4}(U) + K_{L4}h + K_\alpha\alpha \qquad [34]$$

The functions of U are shown on Figure 11. In general, the functions with negative values will not be mirror images of the positive-valued functions. All K's are constant to be determined by test. The effect of increasing velocity is to narrow the wetted flow range of α, which corresponds to the range between the positive and negative limits, and to narrow the width of the hysteresis loop as shown in Figure 12. Increasing the submergence increases the range of α between the limits. This is discussed further in Reference 10.

As may be surmised from Figure 12 cavitation is unlikely to occur on foil panels at lower foil borne speeds unless the foil angle of attack is very large. However, ventilation, which has a similar effect, can occur at these speeds when a foil is surface piercing or is very close to the free surface. When ventilation occurs it is generally assumed to occur down to the first fully submerged fence only. Furthermore, if the foil panel is operating in the portion of the lift curve corresponding to FD of Figure 6 it seems reasonable to assume, as was done in a recent study (9) of a surface piercing hydrofoil boat, that ventilation ceases when a fence goes through the water surface either coming in or going out.

The operation of the control equations can be given in a series of steps stated as instructions:

1. Start the process by choosing a C_L which is either C_{Lw} or C_{Lc} but which is consistent with the initial conditions of the craft.

2. Compare C_L with C_{L+DL}.

   a. If $C_L \leq C_{L+DL}$, go to step 3.

   b. If $C_L > C_{L+DL}$, go to step 5.

3. Compare C_L with C_{L-IL}

   a. If $C_L \geq C_{L-IL}$, select $C_L = C_{Lw}$.

   b. If $C_L < C_{L-IL}$, go to step 4.

4. Compare C_L with C_{L-DL}

   a. If $C_L < C_{L-DL}$, select $C_L = C_{Lc}$.

   b. If $C_L \geq C_{L-DL}$, go to step 6.

5. Compare C_L with C_{L+IL}

   a. If $C_L > C_{L+IL}$, select $C_L = C_{Lc}$.

   b. If $C_L \leq C_{L+IL}$, go to step 6.

6. Check: was $C_L = C_{Lw}$ at $(t-\Delta t)$*

   a. If "NO," go to step 7.

   b. If "YES," select $C_L = C_{Lw}$.

---

* The expression $(t-\Delta t)$ refers to a point in time an instant prior to present time, t. On a digital computer the interval, Δt, would probably be specified; on an analog it is implicit in the mechanization of the problem through the use of relays.

7. Check: Is submergence** of fence at upper end of segment positive?
   a. If "NO," select $C_L = C_{Lc}$.
   b. If "YES," select $C_L = C_{Lw}$.

Note that step 6 is necessary to account for the fact that results at any instant depend on past events. That is to say, it constrains the potential ambiguity associated with the hysteresis loop. It is important to realize that all of the preceding discussion on "lift coefficient" applies separately to each foil and strut on a hydrofoil vehicle. Thus, if a particular craft has four foils and three struts each of the previous equations must be repeated seven times with the correct functions operating for each individual foil and strut.

2. Effect of Unsteadiness - Since the boat motions are in general unsteady the pressure distributions on the lifting surfaces do not adjust themselves instantaneously to the steady state values corresponding to the actual operating conditions prevailing at each instant. In general there is a time lag. This is often expressed in terms of the indicial admittance of the hydrofoil which is represented by a curve of lift versus time following a step change in angle of attack (see Reference 5). For hydrofoils of aspect ratio 6 the lift starts at above 60 percent

---

** If there is no fence it is assumed that the submergence is not positive.

of the steady value and reaches 95 percent of this value in about 4 chord lengths of travel. This unsteady effect diminishes with decreasing aspect ratio. For surface piercing foils one should ideally take into account the effect of varying aspect ratio. However, as a practical matter an average aspect ratio may be assumed. Furthermore, it has been considered satisfactory to approximate the indicial admittance by a sum of a constant and exponentials in time, or even by a first order time lag (4)(5). Recent studies (9) of the effect of the delay in lift change on the motions in waves of a specific hydrofoil craft with aspect ratio 6 hydrofoils have shown them to be unimportant. In an earlier study (11) it was shown that although, in some cases, the major forces on the foils of a subcavitating surface piercing V-foil boat were reduced by as much as 40 percent in head seas, due to lag in lift build up, this did not have a large effect on the motions. However it is possible that the effect would be significant with other configurations.

In most cases the unsteady effect may adequately be represented by a first order lag so that the lift coefficient variation is given by the following differential equation

$$\tau \frac{d\Delta C_L}{dt} + \Delta C_L = \Delta(C_L)_R \qquad [35a]$$

where

ΔC_L is the incremental change in the actual lift coefficient,

$(C_L)_R$ is the incremental change in the lift coefficient computed as if there were no unsteady effect, and

τ is a time constant which depends principally on aspect ratio. (Methods for determining τ are given in Reference 5).

In transfer function form this equation becomes

$$\frac{\Delta C_L}{\Delta (C_L)_R} = \frac{1}{\tau s+1} \qquad [35b]$$

where s is the Laplace transform variable. The equation for the lift coefficient is then the initial lift coefficient $(C_L)_i$ plus the change in lift coefficient

$$C_L = (C_L)_i + \frac{\Delta (C_L)_R}{\tau s+1} \qquad [35c]$$

3. Effect of Added Mass - The added mass of the water associated with the foils and struts has the effect of increasing the effective mass and moment of inertia of these elements. Thus when a foil accelerates in quiet water a retarding force in phase with this acceleration is exerted by the water in the opposite direction. Furthermore, this force is proportional to the relative acceleration experienced by the foil, so that the effect of

accelerations of the water resulting from the orbital particle motion associated with waves can produce both accelerating or retarding effects. In the absence of experimental data the following method may be used for estimating this effect. The resultant force on a foil is assumed to act normal to the foil planform area and is equal to the product of the added mass of the foil and the component of acceleration, at its center of force, which is normal to the planform area. Thus, for the starboard strut we have

$$A_{ss} = -(m_1)_{ss}\ \dot{w}_{ssf} \qquad [36]$$

where

A_{ss} is the force due to added mass effects,

$(m_1)_{ss}$ is the added mass of the ss panel (5), and

$\dot{w}_{ssf}$ is the component of relative acceleration normal to the panel (see below).

According to Equations [15] and [16] we have

$$\dot{w}_{ssf} = -(\dot{v} + \dot{r}\ x_{ss} - \dot{p}z_{ss} - \dot{v}_{ss}' - \dot{v}_{ss}'')\ \sin \Gamma_{ss}$$

$$+ (\dot{w} + \dot{p}y_{ss} - \dot{q}x_{ss} - \dot{w}_{ss}' - \dot{w}_{ss}'')\ \cos \Gamma_{ss} \qquad [37]$$

where

$\dot{v}_{ss}'$ and $\dot{w}_{ss}'$ are given in the last section and

$\dot{v}_{ss}''$ and $\dot{w}_{ss}''$ may be estimated by the methods given in Reference 5*.

Since the force A_{ss} acts parallel to $\dot{w}_{ssf}$, which in turn is positive in the direction of the unit vector $\vec{k}_f$ in the foil axes, its body axis components are obtained with the aid of the matrix in Equation [13], i.e.,

$$\left.\begin{aligned} X_{Ass} &= 0 \\ Y_{Ass} &= (m_1)_{ss} \sin \Gamma_{ss} \dot{w}_{ssf} \\ Z_{Ass} &= -(m_1)_{ss} \cos \Gamma_{ss} \dot{w}_{ssf} \end{aligned}\right\} \qquad [38]$$

Usually the added mass terms $(m_1)_{ss}$, $(m_1)_{sf}$, etc and their moments add up to a rather modest fraction of the total mass and inertia of the boat and their effect on the boat motions is not great. Recent studies of this effect, which were made on a surface piercing hydrofoil boat (9), indicated that the added mass effect on the craft motions was small, producing only minor changes in the peak accelerations.

---

* See footnote to Equation [15].

4. Drag Coefficient - A general expression for the drag coefficient for a hydrofoil with flaps is given in Reference 5. Although it is necessary to obtain the terms that make it up from experimental data the general characteristics of this expression are common to most hydrofoils. The variation of drag coefficient with angle of attack and flap angle is basically parabolic as shown in Figure 13a and 13b. The dominant effect of cavitation or ventilation is to shift this basic curve in the manner shown in Figure 13a. The drop in the drag is associated with the unwetting of one surface. The effect of flap angle, as shown in Figure 13b, can be represented as the sum of the effect of a horizontal shift and the effect of a vertical shift of the position of the basic curve. The horizontal shift may be represented by an increment $\Delta\alpha$ as shown in Figure 14a and the vertical shift by the increment ΔC_D as shown in Figure 14b. Although the effect of submergence on the variation in drag coefficient of fully submerged foils is usually not large over the permissible range of foil depths, this is not so for struts and surface piercing foils because of the significant effect of changing aspect ratio on the drag coefficient (see Reference 5). Generally, this effect can be taken into account with sufficient accuracy by multiplying the drag coefficient by a factor g(h), determined experimentally at a fixed α and δ as a function of depth (see Figure 14c).

Two equations will summarize the functional relationships for the foil drag coefficient. One will apply for fully wetted flow and one for cavitated or vented flow. The control equations

already presented for foil lift coefficient will also control the selection of the foil drag coefficient equation which applies at any instant. For wetted flow

$$C_{Dw} = [g_w(\alpha-\Delta\alpha_w) + \Delta C_{Dw}]g_w(h) \qquad [39]$$

For cavitated or vented flow

$$C_{Dc} = [g_c(\alpha-\Delta\alpha_c) + \Delta C_{Dc}]g_c(h) \qquad [40]$$

where such functions as $g_w(\alpha-\Delta\alpha_w)$, $\Delta\alpha_w$, ΔC_{Dw}, $g_w(h)$ etc. are obtained by fitting to curves such as Figures 13 and 14. It is emphasized that, as with the discussion on lift coefficient, the above presentation, which was adapted from Reference 3b is in some ways arbitrary and that other suitable formulations are possible. However, the guide line in any format is the importance of realism in the representation.

5. Estimation of Hydrodynamic Coefficients - It is well known (5) that there exists a large body of theory and experimental data on both hydrofoils and aircraft lifting surfaces which have been used in the past for deriving methods of estimating the dependence of foil and flap lift, drag and moment on angle of attack, speed, submergence etc. Although these methods are adequate when applied within the limits of the theory and the data on which they are based they are not reliable when extended beyond this range, since they usually do not adequately describe

many important phenomena such as the occurrence and effects of partially and fully cavitated and vented flows, the non-linear variations of lift with angle of attack, the interference effects at foil to foil and foil to strut junctures, the effect of spanwise variation in depth of surface piercing foils and the effect of spanwise variation in side slip angle and angle of attack. It is recognized however, that it will sometimes be necessary to estimate the hydrodynamic coefficients when there is no data on the specific foil of interest available. When this is the case methods such as those given in Reference 5 and 10 can be used.

G. Hydrodynamic Moment Coefficients

The contributions of a foil segment or strut to the moment on the boat, $\vec{Q}_f$, is given by the following vector equation

$$\vec{Q}_f = \vec{r}_f \times \vec{F}_f + \vec{B}_f \qquad [41]$$

where

$\vec{Q}_f = (K_f, M_f, N_f)$. The components are given in boat body axes,

$\vec{r}_f = (x_f, y_f, z_f)$ is the position vector of the center of force of segment f, relative to the boat C.G.,

$\vec{F}_f = (X_f, Y_f, Z_f)$ is the force vector on segment f, with components in boat body axes,

$\vec{B}_f = (k_f, m_f, \eta_f)$

(k_f, m_f, η_f) represent vector components in foil axes of pure couple contributions about the center of force position of each segment. The segments should be selected to make these terms negligible if possible.

$\vec{B}_f$ is generally negligible. However there may be cases where its effect may be considered significant. Contributions to k_f might include roll damping due to roll angular velocity of a segment or foil about a roll axis through its own center of force, effects of sideslip β_f on completely submerged foils with sweep and small dihedral but of small enough span to be treated as a single segment. Contributions to m_f might include moment about the aerodynamic center resulting from lift due to camber effects arising both from foil section design and pitch angular velocity about an axis through the aerodynamic center of the segment. Contributions to η_f might result from effects of sideslip β_f and yaw angular velocities on a segment. This last effect is generally much smaller than the others. Additional effects exist but they are of even lesser importance. A fuller description is given in Reference 5. When it is desired to include such terms, in the absence of specific data on the actual force, the analysis and data of Reference 5 may be used.

The components of $\vec{Q}_f$ in the boat body axes are according to Equation [41]

$$\left.\begin{aligned} K_f &= y_f Z_f - z_f Y_f + (K_f)_e \\ M_f &= z_f X_f - x_f Z_f + (M_f)_e \\ N_f &= x_f Y_f - y_f X_f + (N_f)_e \end{aligned}\right\} \qquad [42]$$

where $((K_f)_e, (M_f)_e, (N_f)_e)$ are the components of $\vec{B}_f$ in boat body axes and are obtained by operating on (k_f, m_f, η_f) with the matrix in Equation [13].

H. Aerodynamic Coefficients

It is well known that aerodynamic drag is a significant design factor. But it is probably not as generally appreciated that the other aerodynamic force components and moments can also play an important roll in the stability and motions of a hydrofoil boat especially in the foilborne mode (5). The complicated form of the hull and superstructure of most conventional boats, together with their proximity to the water surface, make it difficult to estimate these forces and moments without the aid of model data. Test data are normally obtained in a wind tunnel (12). The force and moment components are obtained in body axes over a range of drift angles from 0° to 180° for two or more flight conditions, such as trim angle and elevation near take-off speed and at cruise speed. A typical set of test data are shown in Figure 15. The aerodynamic force and moment components are generally given as follows

$$\left.\begin{aligned} X_a &= \tfrac{1}{2}\rho_a V_a^2 S_a\ C_{Xa} \\ Y_a &= \tfrac{1}{2}\rho_a V_a^2 S_a\ C_{Ya} \\ Z_a &= \tfrac{1}{2}\rho_a V_a^2 S_a\ C_{Za} \\ K_a &= \tfrac{1}{2}\rho_a V_a^2 \ell S_a\ C_{Ka} \\ M_a &= \tfrac{1}{2}\rho_a V_a^2 \ell S_a\ C_{Ma} \\ N_a &= \tfrac{1}{2}\rho_a V_a^2 \ell S_a\ C_{Na} \end{aligned}\right\} \qquad [43]$$

where

ρ_a is the mass density of air,

V_a is relative velocity of air,

S_a reference area used in non-dimensionalizing the aerodynamic coefficients,

ℓ reference length used in non-dimensionalizing the moment coefficients, and

C_{Xa}, C_{Ya}, etc. are aerodynamic coefficients obtained from curves such as given in Figure 15.

I. Forces and Moments on Hull

For the case in which the hull touches the water additional terms for each of the components are required to represent the hydrodynamic force and moment on the hull. There is considerable

data from which the X, Z and M components can be obtained as a function of depth, trim and speed for various high speed hull configurations in quiet water (see References 13, 14 and 15 for example). Such data have been used in the determination of the smooth water drag and trim conditions at various speeds up to take-off (3)(16). Reference 3b gives a detailed description of a method for achieving a simulation of the lift, drag and pitching moment acting on a hull in smooth water in terms of a typical set of data. Only a limited amount of data exists (17)(18) for all six components of force and moment as a function of depth, trim, roll, angle and sideslip angle of planing hulls. Furthermore practically all of the available data is for steady state conditions and do not include dynamic effects. Methods of estimating the static and dynamic components in the hullborne state is discussed in a recent report by C. C. Hsu (19) but these results have not been applied to hydrofoil boats. The effect of the hull impacting the crest of a wave, while the craft is foilborne in a sea state, is discussed in Reference 3d. According to this reference, a digital computer program is available which calculates hull impact forces for symmetrical impact. The shortcoming of the method is that an impact which occurs in 0.5 seconds in real time requires about five minutes of computer time for calculation of forces and motions. Some tentative results have been obtained by imposing a typical impact force history computed from this program, on the simulated craft for which the motions were to be determined. However, the results obtained by

such a procedure are considered questionable. A tentative conclusion from these studies, which appears to be confirmed by experience with the PC(H)-1 in rough water, is that the hull of this hydrofoil craft can cut deeply into the crest of a wave and still remain foilborne. This capability is of course very much dependent on the hull design.

The principle considerations in selecting a hull form are wave impact forces, take-off characteristics, hull borne performance and internal arrangement. Since the hydrofoil operates at high speed close to the water surface wave impacts forces are a primary concern. The magnitude of the impact forces depends on the bottom shape of the boat. A prime rule for selecting hull lines is that the resulting form should minimize the product of area and pressure. Some hulls with unusually high dead rise, designed to accomplish this, are the FRESH I and the LITTLE SQUIRT (42). Furthermore, since boats with a fixed foil system usually give extreme stability in the hull borne mode, they can have very slender hulls to minimize water resistance.

J. Forces and Moments on Entire Boat

Since the hydrodynamic forces, L_f and D_f, as determined from Equation [27]* for each foil segment and strut, are obtained in velocity axes relative to the foil segment or strut axes, it is necessary to resolve these into the body axes of the boat where they enter into the equations of motion. The necessary transformation is given by Equation [14] where α_f and β_f on each

---

* It is usually permissible to assume $C_f \approx 0$.

foil element or strut is obtained with the aid of Equations [15]-[18]. To these are added the contributions of the added mass force components (Equations [38]). After this is done each force component is summed over all foil elements and struts. The resulting sums are the hydrodynamic contributions of the foil-strut system to the X, Y and Z terms, in the boat equations of motion [Equation 1]. The contribution of each foil element and strut to the hydrodynamic moment is similarly obtained by summing each component as determined from Equation [42]. If we add to these the contributions of the aerodynamic terms (Equation [43]), those of the propellers (see Equation [44]) and the hull we obtain the complete expressions for X, Y, Z, K, M, N in Equations [1] and [2]. Generally, for propellers with shaft inclined to the body x-axis the thrust is resolved along the x and z axes and the moment arm components are given by the position vector of the propeller center (x_T, y_T, z_T). The moment about the hull CG is then

$$M_T = z_T X_T - x_T Z_T \qquad [44]$$

where

X_T, Z_T are the x and z components of propeller thrust.

Although transverse forces on the propeller due to angle of attack, exist (5), they are usually assumed to be small and have generally been ignored in past simulations except where data on complete propelled hydrofoil models have been used.

On the basis of the above, we may write the following equations for the aero and hydrodynamic forces and moments on the boat

$$\left.\begin{aligned} X &= \sum_f (X_f + X_{Af}) + \sum_p X_T + X_a + X_H \\ Y &= \sum_f (Y_f + Y_{Af}) + Y_a + Y_H \\ Z &= \sum_f (Z_f + Z_{Af}) + \sum_p Z_T + Z_a + Z_H \\ K &= \sum_f (K_f + K_{Af}) + K_a + K_H \\ M &= \sum_f (M_f + M_{Af}) + \sum_p M_T + M_a + M_H \\ N &= \sum_f (N_f + N_{Af}) + N_a + N_H \end{aligned}\right\} \qquad [45]$$

where

$\sum_f$ is summation over all foils and struts,

$\sum_p$ is summation over all propellers,

X_f, Y_f, etc. are contributions due to lift and drag,

X_{Af}, Y_{Af}, etc. are contributions of added mass,

X_T, Z_T, etc. are contributions of the propellers,

X_a, Y_a, etc. are the aerodynamic terms, and

X_H, Y_H, etc. are contributions of hydrodynamic forces on the hull.

IV. EQUATIONS FOR THE SEAWAY

A. Regular Waves

Although better approximations to gravity waves than the sinusoidal one exist it has not been considered necessary to use them in computations of seaway response of hydrofoil boats. The usual approximation for the elevation of a single wave of wave length λ is given by (20)

$$\eta_{\gamma f} = \frac{H_w}{2} \cos \frac{2\pi}{\lambda_w} (x_{\gamma f}' - c_w t) \qquad [46]$$

where H_w is the wave height (crest to trough), λ_w is wave length, c_w is wave celerity and $x_{\gamma f}'$ is the distance of a given point f from a fixed reference measured in the direction of wave propagation. At the position of a foil or strut, with coordinates x_f, y_f, z_f relative to the CG of the boat, the wave elevation is given by

$$\eta_{\gamma f} = \frac{H_w}{2} \cos \left\{ \frac{2\pi}{\lambda_w} \left[\int (\dot{x}_\gamma - c_w) dt + x_{\gamma f} \right] + \varepsilon_w \right\} \qquad [47]$$

where

$x_{\gamma f}$ is the component of the position vector of the foil relative to the C.G. in the direction of wave propagation,

$\dot{x}_\gamma$ is the component of boat speed at the C.G. in the direction of wave propagation with angle ψ_w to the boat axis (see Figure 16), and

ϵ_w is a constant phase angle selected at random.

The velocity component $\dot{x}_\gamma$ is given by the right hand side of Equation [5a] when we substitute $-\psi_w$ for ψ. Thus,

$$\dot{x}_\gamma = u \cos\theta \cos\psi_w + v(\sin\theta \sin\phi \cos\psi_w + \cos\phi \sin\psi_w) + w(-\sin\phi \sin\psi_w + \sin\theta \cos\phi \cos\psi_w) \quad [48]$$

Since v/u and w/u are usually much less than unity and $\cos\theta \approx 1$ the following approximation is usually valid

$$\dot{x}_\gamma \approx u \cos\psi_w \quad [49]$$

The distance $x_{\gamma f}$ is given by the right hand side of Equation [48] when we substitute (x_f, y_f, z_f) for (u, v, w). For θ and ϕ small this yields the following approximation

$$x_{\gamma f} \approx x_f \cos\psi_w + y_f \sin\psi_w \quad [50]$$

The heading angle relative to the wave propagation direction is

$$\psi_w = \gamma + \psi_o - \int_{\psi=0}^{\psi} \dot{\psi}\, dt \approx \gamma + \psi_o - \int_{\psi=0} r dt \quad [51]$$

where the approximation is valid for Φ small. The x_o axis is taken coincident with the x-axis at time zero. Simplifications in Equations [46-51] result for the case that u is constant. Further simplifications occur for $\dot{\psi} = 0$ and ψ_w constant. For head waves $\psi_w = 180^o$ and following waves $\psi_w = 0^o$.

The orbital velocity components are given in the wave axes by

$$u_{\gamma f} = \frac{H_w}{2}\left(\frac{2\pi}{\lambda_w}\right) c_w e^{-2\pi h_f/\lambda_w} \cos\left[\frac{2\pi}{\lambda_w}(x_{\gamma f}' - c_w t)\right]$$

$$= \frac{2\pi}{\lambda_w} c_w e^{-2\pi h_f/\lambda_w} \eta_{\gamma f}$$

$$w_{\gamma f} = \frac{H_w}{2}\left(\frac{2\pi}{\lambda_w}\right) c_w e^{-2\pi h_f/\lambda_w} \sin\left[\frac{2\pi}{\lambda_w}(x_{\gamma f}' - c_w t)\right] \quad [52]$$

where

h_f is the submergence of the center of force on the foil segment or strut (see Equation [19]),

$u_{\gamma f}$ is the horizontal velocity component in direction x_γ, and

$w_{\gamma f}$ is the vertical component, positive down

The orbital acceleration components are

$$\dot{u}_{\gamma f} = -\frac{H_w}{2}\left(\frac{2\pi}{\lambda_w}\right)^2 c_w^2\, e^{-2\pi h_f/\lambda_w} \sin\left[\frac{2\pi}{\lambda_w}\left(x_{\gamma f}' - c_w t\right)\right]$$

$$\dot{w}_{\gamma f} = \frac{H_w}{2}\left(\frac{2\pi}{\lambda_w}\right)^2 c_w^2\, e^{-2\pi h_f/\lambda_w} \cos\left[\frac{2\pi}{\lambda_w}\left(x_{\gamma f}' - c_w t\right)\right] \qquad [53]$$

In the x_o, y_o, z_o coordinates we have for the orbital velocity* components

$$\left.\begin{aligned} u_{wof} &= u_{\gamma f} \cos(\gamma + \psi_o) \\ v_{wof} &= u_{\gamma f} \sin(\gamma + \psi_o) \\ w_{wof} &= w_{\gamma f} \end{aligned}\right\} \qquad [54]$$

These are transformed to the boat body axes with the aid of Equation [3]. Since θ is always small this reduces to

---

* The acceleration components are resolved in the same manner.

$$\begin{vmatrix} \cos\psi & \sin\psi & -\theta \\ \theta\cos\psi\sin\phi - \sin\psi\cos\phi & \cos\psi\cos\phi + \theta\sin\psi\sin\phi & \sin\phi \\ \theta\cos\psi\cos\phi + \sin\psi\sin\phi & \theta\cos\phi\sin\psi - \sin\phi\cos\psi & \cos\phi \end{vmatrix} \begin{vmatrix} u_{wof} \\ v_{wof} \\ w_{wof} \end{vmatrix} = \begin{vmatrix} u_f' \\ v_f' \\ w_f' \end{vmatrix} \quad [55]$$

where (u_f', v_f', w_f') is the orbital velocity vector in boat axes. When it may be assumed that θ and ϕ are very small this equation can be further simplified to the following

$$\begin{vmatrix} \cos\psi & \sin\psi & 0 \\ -\sin\psi & \cos\psi & 0 \\ 0 & 0 & 1 \end{vmatrix} \begin{vmatrix} u_{wof} \\ v_{wof} \\ w_{wof} \end{vmatrix} \approx \begin{vmatrix} u_f' \\ v_f' \\ w_f' \end{vmatrix} \quad [56]$$

B. The Short Crested Sea

Obviously the representation of a seaway by individual sinusoidal waves is not realistic and if relied upon exclusively can give misleading results. As noted in Reference 21 and 22 the surface elevation $\eta(x_o, y_o, t)$ at a point (x_o, y_o) of the ocean for a fully arisen sea may be idealized as a stationary Gaussian process in three dimensions. Following Pierson (23) the surface elevation may be represented by the following stochastic integral

$$\eta(x_o, y_o, t) = \int_0^{\infty} \int_{-\pi}^{\pi} \cos \left\{ \frac{\omega^2}{g} [x_o \cos(\psi_o + \gamma) + y_o \sin(\psi_o + \gamma)] \right.$$

$$\left. - \omega t + \epsilon(\omega, \gamma) \right\} \sqrt{A^2(\omega, \gamma) d\omega d\gamma} \qquad [57]$$

where

ω is the wave frequency,

$\frac{\omega^2}{g} = \frac{2\pi}{\lambda}$ is the wave number (for deep water),

$A^2(\omega, \gamma)$ is the energy spectrum associated with wave surface amplitude, and

$\epsilon(\omega, \gamma)$ is a random phase angle uniformly distributed in the range $(0, 2\pi)$.

Crudely speaking, the ocean surface is regarded as a superposition of an infinite number of sinusoidal waves of all frequencies, travelling in all directions with random phase angles whose amplitude is modulated by the energy spectrum $A^2(\omega, \gamma)$. There exists a number of empirical energy spectra for fully developed seas that have been used in the past. According to Reference 21 and 22 the most widely used has been the Neumann spectrum which is given by

$$A^2(\omega) = K\omega^{-6}\, e^{-2g^2/U_w^2\omega^2} \qquad [58]$$

where

$K = 51.5\ ft^2/sec^5$, is an empirical constant,

U_w = wind speed.

This spectrum has been used in most of the simulations of hydrofoil boat motions carried out in the past (3),(4),(9),(24) and (25). The energy of this spectrum has usually been assumed to be spread directionally over a range of $\pm 90^\circ$ to the wind direction; i.e.,

$$A^2(\omega,\gamma) = \begin{cases} \frac{2}{\pi} A^2(\omega) \cos^2\gamma & -\frac{\pi}{2} \le \gamma \le \frac{\pi}{2} \\ 0 & \text{otherwise} \end{cases} \qquad [59]$$

More recently a spectrum for a fully developed sea, proposed by Pierson and Moskowitz (26), was used as part of a computer program developed at New York University for hind casting the directional spectrum of the waves over the entire North Atlantic using sea level-wind field data, during the year (1959). Because of the good agreement of this formulation with extensive measurements of spectra for fully developed seas obtained by Moskowitz, and because of the good theoretical basis for this spectrum it is believed to be the most realistic representation of a fully developed sea presently available. The form of this spectrum is given by

$$A^2(\omega) = 16.20 \times 10^{-3}\, g^2 \omega^{-5}\, e^{-0.74(g/V_w\omega)^4} \qquad [60]$$

where V_w is the wind velocity 19.5 meters above the sea surface. The area under the spectrum given by Equation [60] is defined to be equal to twice the variance of the wave record. It should be noted that Equation [60] is dimensionally consistent while Equation [58] is not. The directional properties of this spectrum is obtained by spreading the energy $\pm 90^o$ to the wind direction according to

$$F(\omega,\gamma) = \begin{cases} \frac{1}{\pi}\left\{1 + \left[0.50 + 0.82\, e^{-\frac{1}{2}(\omega V_w/g)^4}\right]\cos 2\gamma \right. \\ \left. + \left[0.32\, e^{-\frac{1}{2}(\omega V_w/g)^4}\right]\cos 4\gamma\right\} & \text{for } -\frac{\pi}{2} < \gamma < \frac{\pi}{2} \\ 0 & \text{otherwise} \end{cases} \qquad [61]$$

Equations [50] thru [60] are restricted to a seaway which has reached the fully developed state. This occurs only when the generating wind has blown over a sufficient fetch and time duration, and the surface elevation fluctuations can be considered a stationary ergodic random process. The effect of fetch and duration on the Neumann spectrum is discussed in References 21 and 27.

In recent years it has also become possible to make use of the library of actual hind casted sea spectra in the North Atlantic, mentioned in the previous paragraph. In order to simulate the effect of realistic short crested seas on ship motions Wachnik and Zarnick (28) have recently availed themselves of these data. According to this reference, these spectra are given at each of 519 grid points which represents a square area of the Atlantic Ocean approximately 2 degrees of latitude per side. The changes in wave spectra are predicted at each point every three hours by considering three factors; propagation, dissipation and growth. The propagation factor takes into account the propagation of energy in and out of the grid and automatically accounts for fetch and swell; the dissipation factor takes into account the attenuation of the waves moving in opposite directions to the local wind-generated waves resulting from gross turbulence effects; and the growth factor takes into account the growth of the wave components if they do not correspond to a fully developed sea. The spectral energy was computed in 15 frequency intervals and 12 direction intervals at each point of the grid, every 6 hours, for a period of one year (1959), in addition to 2 months of exceptionally stormy weather. It is important to note that these spectra include not only the effects of locally generated wind waves but also the effects of swell originating at great distances.

Equation [57] may be expressed in terms of the boat motion and the foil or strut position as follows

$$\eta(x_f, y_f, t) = \int_0^{\infty} \int_{-\pi}^{+\pi} \cos\left\{\frac{\omega^2}{g}\left[\int \dot{x}_\gamma dt + x_{\gamma f}\right] - \omega t + \epsilon(\omega,\gamma)\right\}\sqrt{A^2(\omega,\gamma)}\, d\omega d\gamma \qquad [62]$$

Of course when numerical computations are made the integral in the above equation must be approximated by a finite Fourier sum, such as:

$$\eta(x_f, y_f, t) = \sum_{j=1}^{n}\sum_{i=1}^{m} \cos\ \zeta_{ij}\ [A^2(\omega_j \gamma_i)\ \Delta\omega\Delta\gamma]^{\frac{1}{2}} \qquad [63]$$

where

$$\zeta_{ij} = \frac{\omega_j^2}{g}\left[\int \dot{x}_{\gamma_i f} dt + x_{\gamma_i f}\right] - \omega_j t + \epsilon_{ij} \qquad [64]$$

and i and j represent the number of γ values and frequencies used in the summation. Care must be taken in the choice of these intervals so that the wave height energy is distributed over many components to insure a statistically equivalent seaway (see Reference 22). Experience shows (22) that ergodicity seems to be satisfied for spans of time longer than about 50 times the period of the dominant waves.

For the case of straight foil borne flight it is often satisfactory to make the simplifying assumption that the boat velocity is constant. In this case Equation [64] becomes

$$\zeta_{ij} = \frac{\omega_j^2}{g}(x_f \cos\psi_w + y_f \sin\psi_w) - (\omega_e)_{ij}t - \epsilon_{ij} \qquad [65]$$

where

$\psi_w = \gamma_i + \psi_o$ (since $\psi = \psi_{t=0} = 0$ in this case),

$(\omega_e)_{ij} = \omega_j\left(1 - \frac{\omega_j U}{g}\cos\psi_w\right)$ is the frequency of encounter with waves of frequency ω_j and heading relative to the wind γ_i, and

U = constant boat speed.

With the aid of Equation [52], [54] and [63], the orbital velocity components, at a given foil or strut, are readily seen to be, in fixed axes, the following

$$u_{wof} = \sum_{j=1}^{n}\sum_{i=1}^{m}\omega_j \exp\left[-\frac{\omega_j^2 h_f}{g}\right]\cos\zeta_{ij}\cos(\psi_o+\gamma_i)[A^2(\omega_j\gamma_i)\Delta\omega\Delta\gamma]^{\frac{1}{2}}$$

$$v_{wof} = \sum_{j=1}^{n}\sum_{i=1}^{m}\omega_j \exp\left[-\frac{\omega_j^2 h_f}{g}\right]\cos\zeta_{ij}\sin(\psi_o+\gamma_i)[A^2(\omega_j\gamma_i)\Delta\omega\Delta\gamma]^{\frac{1}{2}}$$

$$w_{wof} = \sum_{j=1}^{n}\sum_{i=1}^{m}\omega_j \exp\left[-\frac{\omega_j^2 h_f}{g}\right]\sin\zeta_{ij}\,[A^2(\omega_j\gamma_i)\Delta\omega\Delta\gamma]^{\frac{1}{2}} \qquad [66]$$

The orbital velocity components in the boat axes are obtained by substituting the above in Equations [55] or [56]. For the case of straight foil borne flight, where the simplifying approximations resulting in Equation [56] are usually valid. The orbital velocity components in the boat axes and in the fixed axes are the same since $\psi = 0$ (see Equation [65]).

C. Irregular Long Crested Waves

In most of the studies on the motions of hydrofoil craft in waves which have been carried out in the past it has been assumed that the seaway was unidirectional with a wave length distribution given by the Neumann spectrum. This has the obvious advantage of considerably simplifying the computations. This is especially true when simulating on an analogue computer the wave height and orbital velocity spectra by means of electrical filters and time delay networks. A discussion of this technique is given in Reference 3c. However, although considerable realism can be obtained by this method, important effects, such as rolling in following seas, etc. cannot be determined with this simplified model and care and judgement must be exercised in the interpretation of the results obtained. It is therefore felt that when making studies of boat behavior in a seaway, the simulation of the short crested sea should be used whenever feasible.

V. CONTROL CONSIDERATIONS*

A. Introduction

For the purpose of this report it will be assumed that all hydrofoil craft of interest will be required to operate within prescribed limits of dynamic motions while in rough seas. An example of such a set of requirements for a fully submerged foil system with a canard configuration is given below (25).

Longitudinal Control System Capabilities:

1. Negotiate State 5 seas at all headings.
2. Minimize hull hitting and broaching in the State 5 sea condition.
3. Maintain vertical acceleration at less than .3 g rms using a 9 foot forward strut and .2 g rms using an 11 foot strut when subjected to a State 5 sea.
4. Take-off and land at a relative heading of 90 to 180 degrees in seas state 5 conditions.

Lateral Control System Capabilities:

1. Negotiate and stabilize the craft at all headings in a State 5 sea.
2. Control roll angle within 1 degree at all headings.
3. Maintain lateral acceleration within 0.2 g at all headings.
4. Make coordinated turns in all sea states up to state 5.

---

* Some parts of this section are taken from Reference 3b.

It is generally agreed that completely submerged foil systems have poor depth and roll angle stability at the usual submergences and that some type of automatic dynamic control system is required to achieve the desired performance. Some investigators have found that an automatic control system is necessary even for some area stabilized craft which are inherently stable and capable of operation in a moderate seaway. As an example, the DENISON (29) employed an automatic control system in order to reduce the pitch down tendency of the craft in the following seas and the vertical accelerations in head seas. On the other hand, a hydrofoil boat, recently built for the Royal Canadian Navy, the FHE 400, has been designed to operate in sea states up to and including 5 without the aid of sensors, moving parts, or an auto pilot. According to Reference 30 a 3-ton 1/4 scale manned model can take off and operate successfully at all headings in waves exceeding appreciably a model State 5 sea.

The three ways usually* considered for obtaining the desired response characteristics with controls are: (1) rotating entire foils to give varying angles of attack (incidence control); (2) rotating hinged trailing edge sections of foils (flap control); and (3) rotating an outboard foil section (tip control). For steering control, the struts may be considered as vertical

---

* These are the conventional controls. However there are a large variety of other types of control that can be used. Many of these are described in References 40 and 41.

foils so that steering can be achieved by rotating a strut, by rotating a hinged trailing edge flap, or by rotating an extension of a strut below a foil as is now being done in some cases. In the latter case the rudder is called a "spade" or "ventral" rudder.

When an auto pilot is used the actuation of any of these movable surfaces is commonly accomplished by hydraulic actuators. The actuators are, in turn, controlled by an electro-hydraulic servo-valve. Electrical signals to activate the servo-valve come from the electronics portion of the automatic control system (ACS). This series of components, plus the pilot, motion sensors, and position feedback transducer are shown in Figure 17.

Control signals originate at the pilot's controls, at the motion sensors, and at the position transducer. These are combined and processed in the electronics to produce the signal for the servo-valve. The pilot will be able to move the helm, a lever, or a knob to introduce steering, altitude and attitude commands; the motion sensors sense errors between the commanded and actual craft motions and produce electrical signals proportional to these errors; the position transducer provides the feedback signal so that the control surface stops moving when it has reached the position corresponding to the processed error signals. The composite system indicated by the block diagram of Figure 17 is a typical "control loop," "control channel," or group of "control signal paths."

B. Component Dynamics

The manner in which the effect of the control surface deflections entered the equations of motion through the force coefficients was discussed under the sections entitled "Lift Coefficient and Drag Coefficient." It is now necessary to consider how the control system components affect the equations of motion through the control surface deflections. In general, a signal originating at the pilot or at the motion sensors will be modified by the individual dynamics of the components in the signal path before the control surface motion actually occurs. Inputs by the pilot are considered to be prime signals with no modification to account for the dynamics of the pilot. Motion sensors to be discussed are vertical gyros, rate gyros, accelerometers and height sensors.

Vertical Gyro - A vertical gyro of the type of interest here will produce one signal directly proportional to the pitch angle of the craft and one signal directly proportional to the roll angle of the craft. The instrument introduces no primary dynamic effects. Secondary effects associated with the erection cycle may have to be considered.

Rate Gyros - A rate gyro will sense an angular rate about one of the three body axes. (Three-gyro "rate packages" are available if required for a particular application). The dynamics of the gyro are such as to produce an output signal which is related to the actual angular rate by a second order differential equation. Using the roll rate, p, as an example, the equation is:

$$\frac{1}{\omega_N^2}\left(\frac{d^2\tilde{p}}{dt^2} + 2\zeta\omega_N\frac{d\tilde{p}}{dt} + \omega_N^2\tilde{p}\right) = p \qquad [67]$$

or, in transfer function form for all rotational rates:

$$\frac{\tilde{p}}{p} = \frac{\tilde{q}}{q} = \frac{\tilde{r}}{r} = \frac{\omega_N^2}{s^2 + 2\rho\omega_N s + \omega_N^2} \qquad [68]$$

where

$\tilde{p}$, $\tilde{q}$, $\tilde{r}$ = Outputs of rate gyros (rad/sec),

p, q, r = Craft rotational rates (rad/sec),

ω_N = Natural frequency of a particular gyro (rad/sec),

ζ = Damping ratio of a particular gyro (dimensionless), and

s = Differentiation operator (or Laplace transform variable)(1/sec).

Equipment catalogs list natural frequencies and damping ratios available for these instruments. In the dynamic analysis or simulation of a particular craft, the values used will be those corresponding to the sensor to be installed in the craft. Common values are:

$$\omega_N = 10 \text{ cps} = 2\pi(10) \text{ Rad/Sec}$$

and

$$\zeta = 0.7.$$

Accelerometers - Outputs of accelerometers are also assumed to relate to the craft motions by second order differential equations. In general form, the equation is:

$$\frac{1}{\omega_N^2}\left(\frac{d^2\tilde{a}_i}{dt^2} + 2\zeta\omega_N\frac{d\tilde{a}_i}{dt} + \omega_N^2\tilde{a}_1\right) = a_i \qquad [69]$$

or

$$\frac{\tilde{a}_i}{a_i} = \frac{\omega_N^2}{s^2 + 2\zeta\omega_N s + \omega_N^2} \qquad [70]$$

where i will become a symbol corresponding to the location of a particular accelerometer. Common values for the natural frequency and damping are:

$$\omega_N = 20 \text{ cps} = 2\pi(20) \text{ Rad/Sec}$$

and

$$\zeta = 0.7.$$

To identify the accelerations sensed by the instruments, it will be assumed that there is one accelerometer at the c.g. mounted such as to measure lateral acceleration, and one accelerometer above each foil mounted in the x-y plane so as to measure accelerations parallel to the z-axis.

The lateral acceleration at the c.g. is:

$$(a_y)_{cg} = \frac{Y + mg \cos\theta \sin\phi}{m} \qquad [71]$$

Taking angular accelerations into account, the accelerations in the z-direction at points above a rear, port, and starboard strut are:

$$(a_z)_{rs} = \frac{Z + mg \cos\theta \cos\phi}{m} - x_{rs}\dot{q} \qquad [72]$$

$$(a_z)_{ps} = \frac{Z + mg \cos\theta \cos\phi}{m} + y_{ps}\dot{p} - x_{ps}\dot{q} \qquad [73]$$

$$(a_z)_{ss} = \frac{Z + mg \cos\theta \cos\phi}{m} + y_{ss}\dot{p} - x_{ss}\dot{q} \qquad [74]$$

Height Sensors - To date, height sensors have not been standardized as the other instruments have. Ultrasonic and sonar types are either in use or expected to be used. Semi-submerged resistance wire and multiple pitot pressure types have also been proposed. It can sometimes be assumed that the dynamic characteristics of the sensor will be such as to give a direct

indication of the instantaneous height of the sensor above the water. This assumption has been shown to be reasonable for the ultra-sonic sensor on HIGH POINT and FRESH-1.

Control Electronics - The control electronics comprise a complex subsystem of the complete automatic control system. This subsystem amplifies, combines and modifies the signals it receives and directs the resultant electrical commands to the electro-hydraulic servo valves.

Dynamic performance of a hydrofoil craft with autopilot is strongly dependent upon the control electronics; consequently, a single mathematical description of this subsystem, applicable to all hydrofoils, would be highly desirable. It happens, however, that the manner in which the incoming signals are processed by the circuitry will be unique for each design of hydrofoil craft; this makes a uniform representation impossible. It is possible, however, to subdivide the functions and identify the basic types of operations which the electronics normally perform, and it is possible to write equations which describe these operations.

Three functions of the electronics are: (1) summation, (2) amplification, and (3) signal modification. Signal modifications are necessary in order to give the overall craft the desired dynamic characteristics. The modifications are often called "signal shaping" and their specifications are based on a dynamics analysis of the craft. It is possible for a single component

(amplifier) to simultaneously perform the addition and amplification functions, but for practical reasons, related to implementing the signal modifications, two amplifiers in series are commonly used. In this arrangement the first amplifier in the control path is called the "mixer amplifier"; it performs additions, some amplification, and allows the modification of signals. The second amplifier is called the "driver amplifier"; it adds the position feedback signal and completes the necessary amplification. It is this second amplifier which "drives" the servo valve.

For purposes of presentation of equations, the mixer amplifier, the driver amplifier and the modification circuitry will be treated as separate entities. (During the dynamics analysis and design leading to a complete hydrofoil craft, it is essential that the three be treated as closely integrated and strongly interdependent components.)

The exact mathematical representations for the mixer and driver will vary with particular designs; for preliminary design purposes it will be assumed that the characteristics of each of them can be represented by a first order differential equation in this way:

$$\frac{d\theta_o}{dt} + \frac{1}{\tau}\theta_o = \frac{1}{\tau}\Sigma\,\theta_1 \qquad [75]$$

where

θ_o = the signal out of the amplifier,

$\Sigma\theta_i$ = the sum of all input signals, and

τ = characteristic time constant of the particular amplifier.

In Laplace variable and transfer function notation, this is:

$$\frac{\theta_o}{\Sigma\theta_i} = \frac{1/\tau}{s + \frac{1}{\tau}} \qquad [76]$$

The signal modification circuitry probably constitutes the most widely variable segment of the equation development. Each signal is subject to an essentially limitless number of modifications in addition to the operations of amplification and addition previously mentioned. Although the number of possible modifications is limitless, the modification of a particular signal can usually be represented by this general equation:

$$a_o\theta_o + a_1 \frac{d\theta_o}{dt} + a_2 \frac{d^2\theta_o}{dt^2} + \ldots a_m \frac{d^m\theta_o}{dt^m} = b_o\theta_i$$

$$+ b_1 \frac{d\theta_i}{dt} + b_2 \frac{d^2\theta_i}{dt} + \ldots b_n \frac{d^n\theta_i}{dt^n} \qquad [77]$$

where

θ_1 and θ_o are circuit input and output signals, respectively,

a's and b's are constant, and

$m > n$.

In transfer function form this becomes

$$\frac{\theta_o}{\theta_i} = \frac{b_o + b_1 s + b_2 s^2 + \ldots b_n s^n}{a_o + a_1 s + a_2 s^2 + \ldots a_m s^m} \qquad [78]$$

which is factorable to

$$\frac{\theta_o}{\theta_1} = \frac{(s + z_1)(s + z_2) \ldots (s + z_n)}{(s + p_1)(s + p_2) \ldots (s + p_m)} \qquad [79]$$

where any two z's and any two p's may be complex conjugates and any z or p may be zero. The net effect of circuits of this type is to shape a signal's dynamic characteristic in the frequency domain. A signal, so modified, can experience an amplification at certain selected frequencies and attenuation at others. This process is sometimes termed "compensation." The initial selection of the form of these transfer functions is generally determined from a preliminary control study based on the linearized equations of motion of the boat (1).

The servo portion of the control loop (Figure 17) remains to be considered.

Servomechanism - The electro-hydraulic servo valve, hydraulic actuator, position transducer, and summing function of the driver amplifier combine to form a servomechanism, or more usually simply a "servo." The dynamic characteristic of these parts, taken as a unit, can usually be acceptably represented by a first order differential equation, thus:

$$\frac{d\delta}{dt} + \frac{1}{\tau}\delta = \frac{1}{\tau}\delta_C \qquad [80]$$

where

δ = control surface deflection,

δ_C = commanded deflection, and

τ = characteristic time constant.

As a transfer function, this is written:

$$\frac{\delta}{\delta_C} = \frac{1/\tau}{s + \frac{1}{\tau}} \qquad [81]$$

The control equations for a representative control loop and the manner in which they combine are summarized in Figure 18, where it has been assumed that the transfer functions of the height sensor and vertical gyro are unity.

C. Preliminary Control Study

Assumptions - It has been customary to first carry out a preliminary design of the control system by means of linear control system synthesis procedures and then to use the results of this study in the computer simulation of the complete non-linear problem. In order to carry the first part of this process out the following assumptions are usually made:

1. The equations of motion of the boat are linear so that the longitudinal and lateral equations are uncoupled (see Reference 1). This allows one to carry out a preliminary design of the longitudinal control system independently of the lateral system. However, since the stability will depend on the craft trim, depth and speed it will be necessary to investigate the longitudinal and lateral stability and control over a range of operating conditions. This may include some extreme conditions of strut immersion if the craft is to operate in a heavy sea (4).

2. Unsteady hydrodynamic effects are negligible. This is not a necessary assumption and was not made in Reference 4. Nevertheless, it is generally a permissible one to make. However, this effect should be included in the response to seaway determinations.

3. The craft is infinitely stiff; i.e., the structural natural frequencies are high in comparison with the operating frequencies of the control surface. This effect should be examined in more detail in later stages of the analysis, especially if any of the primary structural natural frequencies are not considerably larger than the maximum wave encounter frequencies.

Comparisons made in Reference 4, for example, of the calm water behavior of a completely submerged hydrofoil configuration obtained on the basis of the linearization assumption, with that obtained from a complete computer simulation, in which the non-linearities were included, showed no radical discrepancies. It is therefore feasible, as with aircraft, to obtain a good preliminary design of the control system by means of existing linear procedures such as the root locus method, Nichols charts, method of non-interacting controls, etc. Once this is done, the task of optimizing the design by means of a computer simulation, which includes the non-linearities of the system, such as effects of cavitation and ventilation, wetted area changes, control rate and angle limiting, etc. are considerably simplified.

Inputs - The control system in general has to be designed to perform well with respect to three principle types of inputs - no inputs, disturbance inputs and command inputs. No inputs leads to a stability problem. Disturbance inputs, such as those due to waves, leads to a stabilization problem; i.e., the ability of the craft to maintain the desired flight in spite of external forces and moments applied to it. Command inputs lead to a maneuvering problem. These are discussed further below.

Stability - Although completely submerged fully wetted foil systems are usually stable due to the increase of foil lift with depth of submergence this effect is too small to prevent excessive transient motions without some type of height and pitch feedback to flap and elevator. Transverse motions are unstable

due to roll-sway coupling. This is discussed in Reference 31. The coupling of sway and roll into yaw is usually relatively small compared with the coupling between sway and roll. A positive sway, for example, creates a positive roll due to the positive roll moment, $K_v'v'$, generated by the struts. This in turn produces an increase in the positive sway motion. The resultant instability is evidenced by the negative value of the last constant E in the characteristic quartic equation for inherent lateral stability. This is given by the following equation from Reference 31:

$$E = E_1 + E_2 + E_3 \qquad [82]$$

where

$$E_1 = (Y_\phi' + C_{Lo})(K_v'N_r' - N_vK_r') < 0$$

$$E_2 = -K_\phi' [Y_v'N_r' + N_v'(m'-Y_r')] \approx 0$$

$$E_3 = N_\phi' [K_v'(m'-Y_r') + Y_v'K_r'] \approx 0$$

for completely submerged foils. Since N_r' in E_1 and Y_v' in E_2 are large and negative it is seen that the principle cause of the instability is the large positive value of K_v' and the small negative value of K_ϕ'. Although K_v' can be reduced by dihedral and sweep on the hydrofoils it is extremely unlikely that stability could be achieved by this means for a completely submerged foil system. It appears that roll angle feedback to

the ailerons would be required to compensate, for the small K_{ϕ}' and help make the craft stable.* However if a substantial reduction in K_{v}' is possible it can be of benefit in relieving the demands on the ailerons by delaying the onset of saturation effects with the consequent deterioration in stability and control. Conceivably the control effectiveness and hence turning performance may be improved in two ways; first due to a reduction of the aileron angle required to maintain a given equilibrium turn and second a reduction in the amount of aileron angle needed to maintain stability. The degree of improvement of course must be determined by detailed analysis. It should be emphasized however, that it is as important to optimize the boat design for good dynamic performance in a seaway as well as the control system.

Stabilization - The principal stabilization problem is to keep the vertical accelerations to a minimum and to prevent hull hitting and foil broaching. If the expected heights of all waves encountered are less than the strut length then an optimum control system would be one that minimizes the vertical motion of the craft, as shown in Figure 19a. However, in a State 5 sea, for example, where 1 out of 10 waves is about 13 feet high and occasionally a wave will reach 17 feet some wave contouring is required to prevent hull hitting and broaching with boats having struts of say 10 feet in length. Furthermore, the contouring

---

* According to Reference 4 there are conditions where a yaw rate-rudder loop is also required to maintain stability.

should be in phase with the wave motion as much as possible. This is graphically illustrated by Figure 19b. Another factor to consider is the relative frequency of encounter. For a given amount of contouring (or percent contouring), the shorter wavelengths (higher frequency of encounter) give higher accelerations. The relationship between wavelength, wave height, percent contouring and the resultant g loads at the foil is shown graphically in Figure 20 for 400 and 200 ft. wavelengths in a head sea. These are typical lengths of high waves for a State 5 sea (21). Assuming that foil motion is in phase with wave motion, the short dotted line indicates the percent contouring (also minimum possible g loads) required to negotiate a given wave height allowing for 8 or 10 ft. of foil depth change. If it is assumed that a minimum allowable foil depth of 1 ft. is required to maintain lift, these dotted lines would correspond to the amount of foil contouring necessary to avoid hull hitting or sudden loss of lift (broaching) with 9 or 11 ft. struts, respectively. Thus we see, for example, that a 17 ft. by 400 ft. wave can theoretically be negotiated without exceeding 0.5 g using a 9 ft. strut, a 14.5 ft. by 400 ft. wave can be theoretically negotiated without exceeding .25 g on 11 ft. strut, etc. However, to achieve perfect contouring of these long waves, requires considerable wave height anticipation. For the linear case, since the force amplitude is 180° out of phase with the displacement, the control force would have to be applied one half wavelength in advance. Although existing sensors, which measure boat height from the instantaneous free water surface, cannot achieve this, definite improvement appears to be

possible with a lead network immediately following the height sensor mounted as far forward as possible (4). Since it is not necessary, nor indeed desirable to contour the short high frequency waves the height sensor signal is put through a first order lag filter. Integral height error is also used to insure steady state accuracy. In addition a rapid response acceleration loop can provide means for attenuating incipient heave accelerations, due to orbital motions, by appropriate flap deflections.

Maneuverability - The maneuvering performance requirements in the vertical plane are secondary to stabilization requirements. The only requirement on the response to commands is due to the limited maneuvering space above the water surface. This requires that there be no overshoot, in the response to height or pitch angle command, which could lead to foil broaching or hull slamming. In transverse motions the maneuvering requirements are more specific. The boat must be able to make both flat and coordinated turns. A flat turn is performed with zero roll angle and is required in the roughest sea conditions to prevent broaching or slamming. Coordinated turns are performed primarily in mild sea conditions where the roll angle increases with heading rate to provide comfortable riding conditions. A more detailed discussion is given in Reference 31.

Methods of Analysis - The linearized preliminary design of the control system has been carried out in the past by the various classical methods described in the literature (32-36). The method using Nichols charts was employed in the study described in References 4 and 7 on the control system design for

fully submerged foil systems. The root locus approach was used in the control studies described in References 25, 37 and 38. The method of non-interacting controls was used in References 24 and 39. Since this last one is not as well known as the others, a brief description is given here. The procedure is an application to hydrofoil boats, of the technique of matrix diagonalization for simplifying multi-coupled systems (36) for the purpose of obtaining a non-interacting system. In a non-interacting system there is a deliberate division of the feedbacks to the control surface in such a fashion that the variables of the problem are made independent; i.e., the motions are decoupled. Thus each variable has its own separate response equation which can be adjusted independently of the other problem variables. It is hoped that by this method adverse coupling effects can be minimized. This is especially desirable due to the limited maneuvering space available in the vertical plane. Although much research has been done in the area of modern optimal control theory, it does not appear that these results have yet found application in hydrofoil autopilot design. A good review of this subject is given in Reference 35.

REFERENCES

1. Martin, M., "Equations of Motion for Hydrofoil Craft," HYDRONAUTICS, Incorporated Technical Report 001-9, 1962.

2. "Nomenclature for Treating the Motion of a Submerged Body Through a Fluid," Technical and Research Bulletin No. 1-5, SNAME, N. Y., April 1950.

3. "Hydrofoil Simulation Equations Study," by the Boeing Company, Seattle, Washington for Naval Training Device Center, Orlando, Florida, under Contract N61339-1630, Project No. 7669-1, December 1966.

   (a) Jamieson, J. J., and Farris, W. E., "Performance Criteria and Test Report for Hydrofoil Craft," NAVTRADEVCEN Technical Report 1630-1.

   (b) Jamieson, J. J., "Mathematical Model Report, Vol 1 and 2," NAVTRADEVCEN Technical Report 1630-2-1, and 1630-2-2.

   (c) Farris, W. E., "Mathematical Model Report, Vol. 3," NAVTRADEVCEN Technical Report 1630-2-3.

   (d) Jamieson, J. J., "Final Report" NAVTRADEVCEN 1630-3.

4. "Engineering Summary Report on a Hydrofoil Autopilot System Design Study Program," by Radio Corporation of America, Burlington, Mass. for Bureau of Ships, Code 456C, Under Contract NObs-84498, Index Number SF 0130201, Task 1709, January 1962 and August 1963.

5. Martin, M., "The Stability Derivatives of a Hydrofoil Boat," Parts I and II, HYDRONAUTICS, Incorporated Technical Report 001-10 (I) and 001-10 (II), January 1963.

6. Imlay, F. H., "Theoretical Motions of Hydrofoil Systems," NACA Report 918, 1948.

7. Connors, J. L., Mass. Institute of Technology, Flight Control Laboratory, Report FCL-7203-R11, May 1955, CONFIDENTIAL.

8. Ogilvie, T. F., "The Theoretical Prediction of the Longitudinal Motions of Hydrofoil Craft," J Ship Research, Vol. 3, No. 3, pp 29-40, December 1959.

9. Davis, B. V. and Oates, G. L., "Hydrofoil Motions in a Random Seaway," DeHavilland Aircraft of Canada, Limited, Downsview, Ontario, Canada, August 1964.

10. Barr, R. A., "Hydrodynamics of Hydrofoil Craft: Chapt. I Cavitation Inception on Foils Struts and Pods. Chapt. III Ventilation Inception of Surface Piercing and Submerged Foils and Struts. HYDRONAUTICS, Incorporated Technical Report 463-1, 1964.

11. Ogilvie, T. F., "The Theoretical Predictions of the Motions of a Hydrofoil Craft," David Taylor Model Basin Report 1138, 1958.

12. Ryan, Earl F., "Aerodynamic Characteristics of a Hydrofoil Craft for Two Operating Attitudes," David Taylor Model Basin Aero Report 965, September 1959.

13. Clement, E. P. and Blount, D. L., "Resistance Tests of a Systematic Series of Planing Hull Forms," SNAME Transactions, Vol. 71, 1963.

14. Benen, Lawrence," General Resistance Test of a Stepless Planing Hull with Application to a Hydrofoil Configuration," David Taylor Model Basin Report 2006, July 1965.

15. Clement, Eugene P., "The Development of Efficient Hull Forms for Hydrofoil Boats," David Taylor Model Basin Report 2160, March 1966.

16. Barr, R. A., "Hydrodynamics of Hydrofoil Craft, Chapt IV Trim, Altitude and Pre-Takeoff Resistance of Hydrofoil Craft," HYDRONAUTICS, Incorporated Technical Report 463-1, 1964.

17. Savitsky, D., Prowse, R. E., and Lueders, D. H., "High-Speed Hydrodynamic Characteristics of a Flat Plate and 20° Dead-Rise Surface in Unsymmetrical Planing Conditions," NACA TN 4187, 1958.

18. Smiley, R. F., "A Theoretical and Experimental Investigation of the Effects of Yaw on Pressures, Forces, and Moments During Seaplane Landings and Planing," NACA TN 2817, 1952.

19. Hsu, C. C., "On the Motions of High Speed Planing Craft," HYDRONAUTICS, Incorporated Technical Report 603-1, May 1967.

20. Lamb, H., Hydrodynamics, Dover, Publications, New York.

21. Martin, M. and Turpin, F. T., "The Effect of Surface Waves on Some Design Parameters of a Hydrofoil Boat," HYDRONAUTICS, Incorporated Technical Report 001-3, January 1961.

22. Chen, C. F., Auslaender, J. and Chen, F. C., "Mathematical Generation of a Realistic Sea," HYDRONAUTICS, Incorporated Technical Report 001-13, October 1963.

23. Pierson, W. J., "Wind Generated Gravity Waves," Advances in Geophysics, Vol. 2, Ed. by H. E. Landsberg, N. Y., Academic, 1955, p. 93.

24. Harris, H. E., et al, "Autopilot System Study for Hydrofoil Craft," Sperry Piedmont Report No. J.A. 250-0037, Charlottesville, Virginia.

25. Olshausen, R., Bridges, E. C. and Krol, J. G., "Hydrofoil Control Study for Bureau of Ships, Autonetics Report EM-0362-211, June 1962. DDC No. AD427002.

26. Pierson, W. J. and Moskowitz, L., "A Proposed Spectral Form for Fully Developed Wind Seas Based on the Similarity Theory of S. A. Kitaigordskii,"Journal of Geophysical Research, Vol. 69, No. 24, December 1964.

27. Pierson, W. J., Jr., Neumann, G. and James, R. W., "Practical Methods for Observing and Forecasting Ocean Waves by Means of Wave Spectra and Statistics," Hydrographic Office Publication No. 603, Navy Department, Washington, D. C., 1958.

28. Wachnik, Z. G., and Zarnick, E. E., "Ship Motions Prediction in Realistic Short Crested Waves," SNAME Transactions, Vol.73, 1965.

29. Krock, R. C. and Gross, J. G., "Experience with the Hydrofoil Craft DENISON," SNAME Paper 2e, Presented in Seattle, Wash., May 13-14, 1965.

30. Lewis, C. Beaumont," A Hydrofoil Ship for the Royal Canadian Navy," SNAME Paper 2-i, Presented in Seattle, Washington, May 13-14, 1965.

31. Hsu, C. C., "Lateral Stability and Control of Hydrofoil Boats," HYDRONAUTICS, Incorporated Technical Report 463-9, November 1967.

32. D'Azzo, J. J., and Houpis, C. H., "Feedback Control System Analysis and Synthesis," McGraw Hill Book Company, N. Y. 1960.

33. Truxal, J. G., "Automatic Feedback Control System Synthesis," McGraw Hill Book Company, 1955.

34. Gille, J. C., Pelegrin, M. J. and Decaulne, P., "Feedback Control Systems," McGraw Hill Book Company, N. Y., 1959.

35. Merriam, C. W., III, "Optimization Theory and the Design of Feedback Control Systems," McGraw Hill Book Company, N. Y., 1964.

36. Boksenbom, A. S. and Hood, R., "General Algebraic Method Applied to Control Analysis of Complex Engine Types," NACA Report 980, 1950.

37. Chuck, G., Luke, R.K.C. and Scroggs, S.J., "Study of Hydrofoil Stability and Control," Hughes Aircraft Company Report SRS-399, Contract NObs-78572, December 1960.

38. Chuck, G. and Luke, R.K.C., "Longitudinal Stability and Control of Canard Hydrofoil Craft," Hughes Aircraft Company Report SRS-440, Contract NObs-78572, June 1961.

39. Noble, T. F., Harris, H. E. and Williams, V. E., "On the Stability and Stabilization of Craft Supported by Fully Submerged Hydrofoils," SNAME Paper presented at the Southern California Section, October 8, 1960.

40. Beason, C. and Buckle, A. K., "Hydrofoil Vessels," Hovering Craft and Hydrofoils, Vol. 5 No. 6, March 1966.

41. Hayward, Leslie, "The History of Hydrofoils," Hovering Craft and Hydrofoil, Vol. 6, No. 2, November 1966.

42. Myers, G. R., "Observations and Comments on Hydrofoils," SNAME Paper No. 2a, Presented in Seattle, Washington, May 13-14, 1965.

TABLE 1

Designation of Segment Forces and Moment Arms

Segment Name	Symbol for Force Components in Body Axes			Symbol for Components of Moment Arms to CG		
Starboard Foil	X_{sf}	Y_{sf}	Z_{sf}	x_{sf}	y_{sf}	z_{sf}
Port Foil	X_{pf}	Y_{pf}	Z_{pf}	x_{pf}	y_{pf}	z_{pf}
Starboard Dihedral	X_{sd}	Y_{sd}	Z_{sd}	x_{sd}	y_{sd}	z_{sd}
Port Dihedral	X_{pd}	Y_{pd}	Z_{pd}	x_{pd}	y_{pd}	z_{pd}
Starboard Strut	X_{ss}	Y_{ss}	Z_{ss}	x_{ss}	y_{ss}	z_{ss}
Port Strut	X_{ps}	Y_{ps}	Z_{ps}	x_{ps}	y_{ps}	z_{ps}
Starboard Anhedral	X_{sa}	Y_{sa}	Z_{sa}	x_{sa}	y_{sa}	z_{sa}
Port Anhedral	X_{pa}	Y_{pa}	Z_{pa}	x_{pa}	y_{pa}	z_{pa}
Rear Foil	X_{rf}	Y_{rf}	Z_{rf}	x_{rf}	y_{rf}	z_{rf}
Rear Strut	X_{rs}	Y_{rs}	Z_{rs}	x_{rs}	y_{rs}	z_{rs}

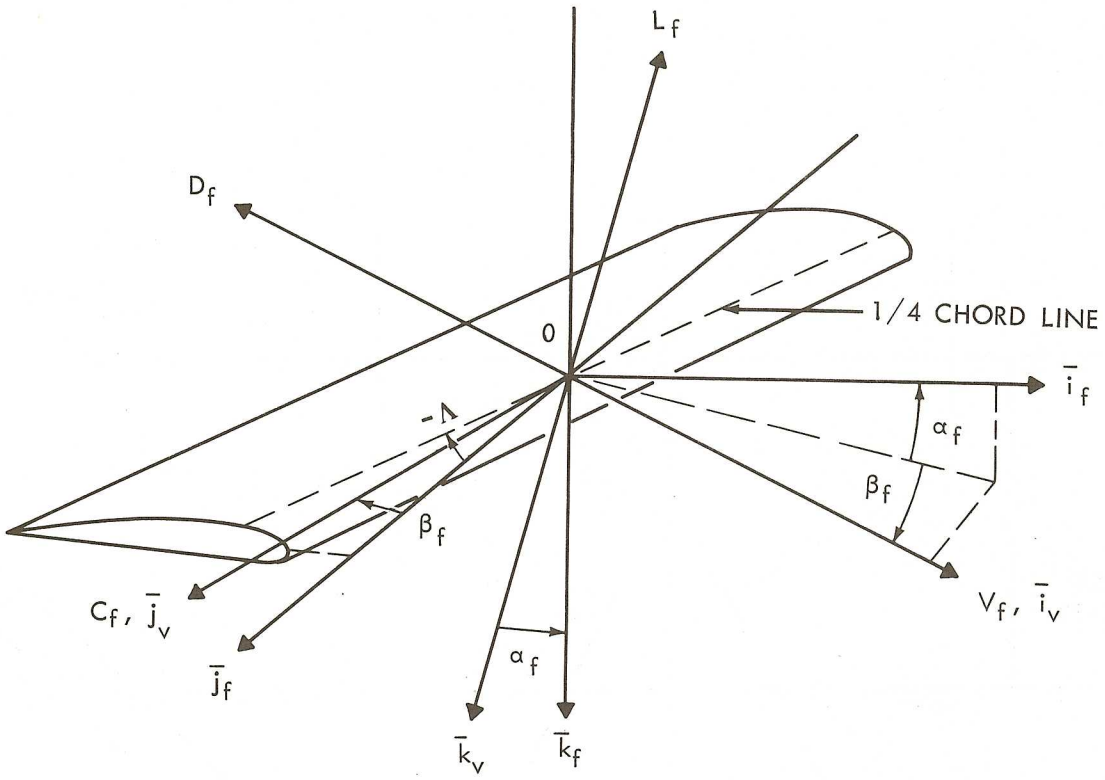

Figure 3 - FOIL VELOCITY AXES RELATIVE TO FOIL AXES

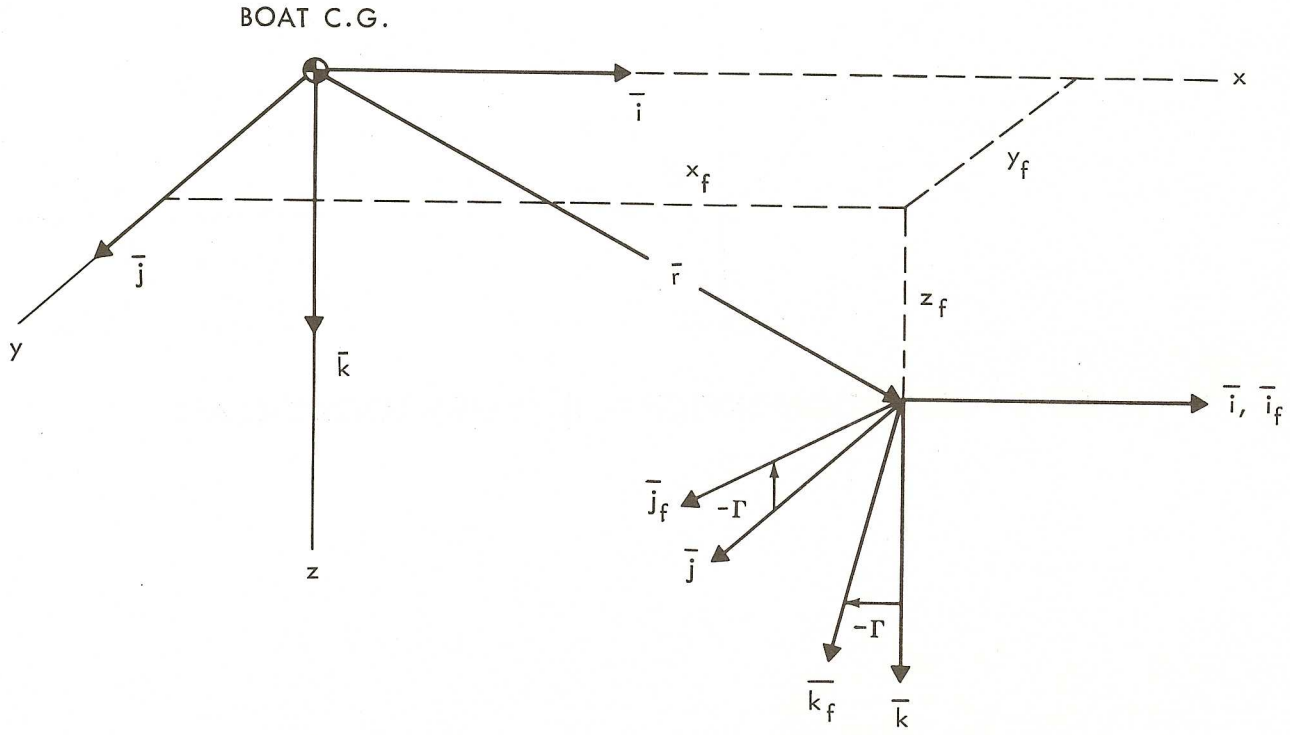

FIGURE 4 - FOIL AXES RELATIVE TO BOAT AXES

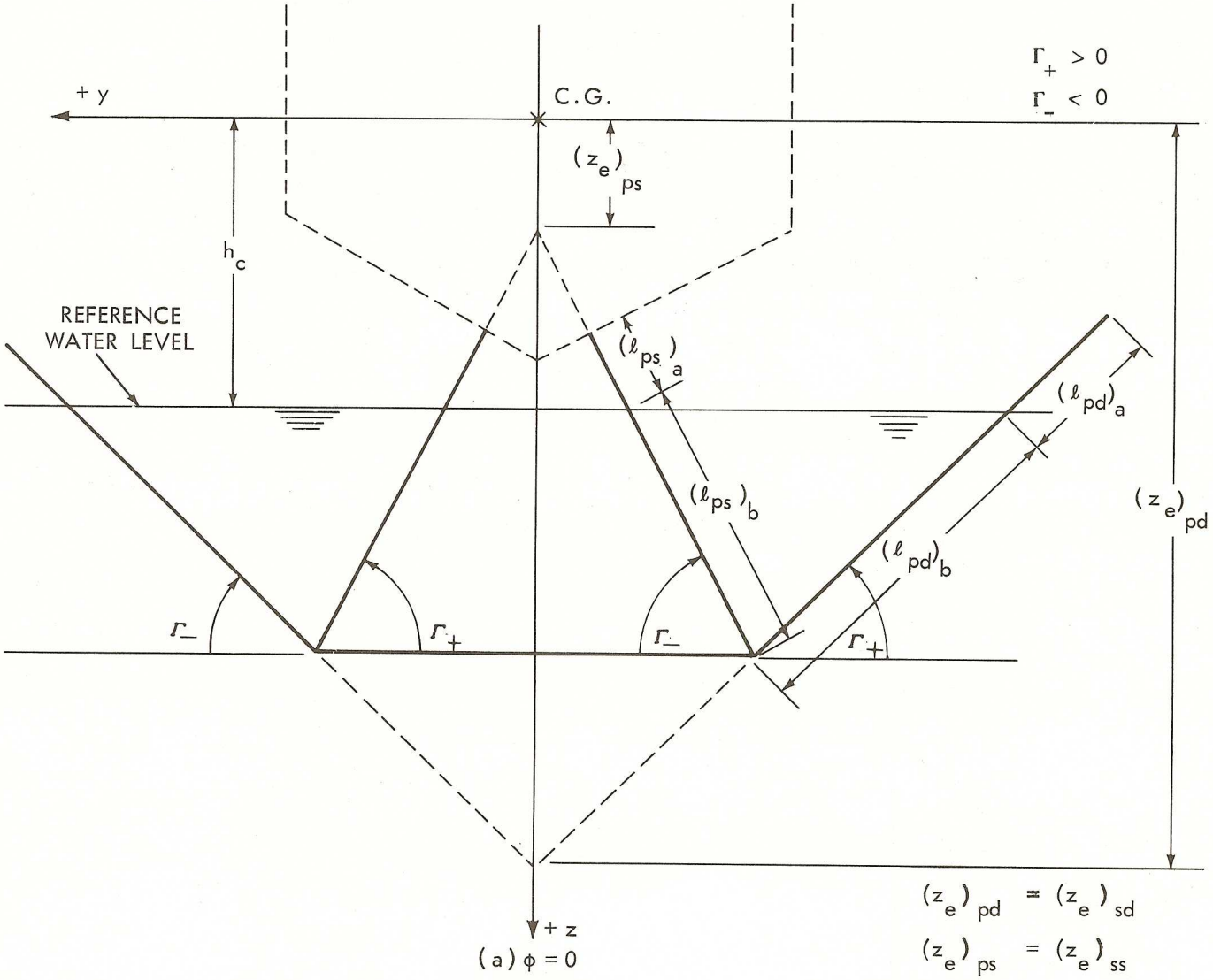

FIGURE 5 - DEFINITION SKETCH FOIL SYSTEM LOOKING AFT

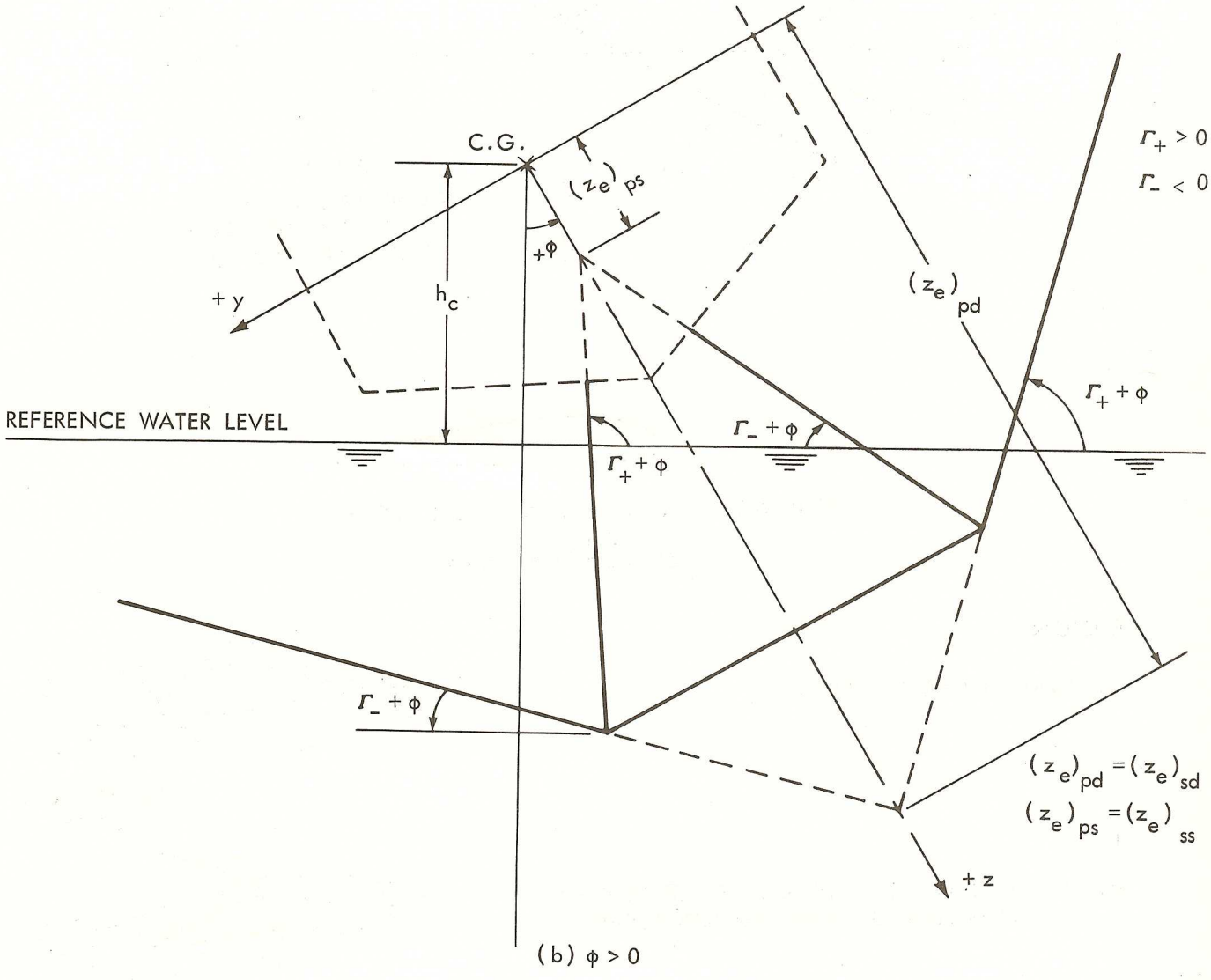

FIGURE 5 - CONCLUDED

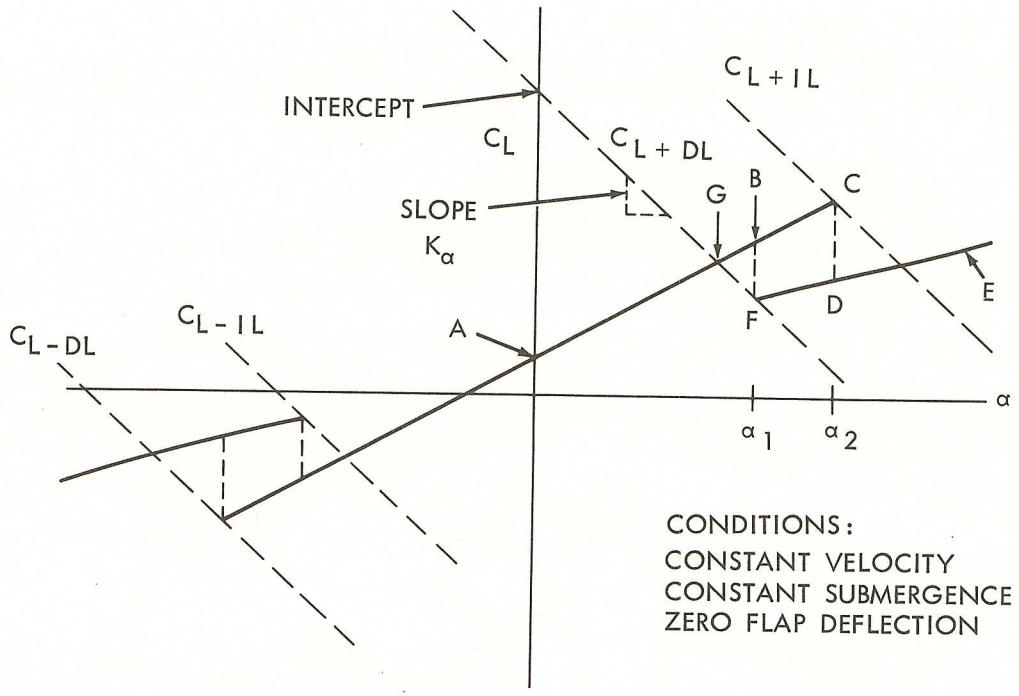

FOIL WITH CONVENTIONAL CROSS SECTION
AND
TRAILING EDGE FLAP

REGION

AB - FULLY WETTED FLOW

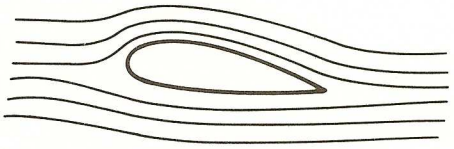

CAVITATION BUBBLES

BCDFG - PARTIALLY CAVITATED AND/OR VENTED FLOW (MIXED OR TRANSITION FLOW)

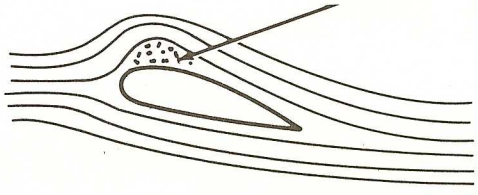

CAVITY

EDF - FULLY CAVITATED AND/OR VENTED FLOW (ANGLE EXAGERATED)

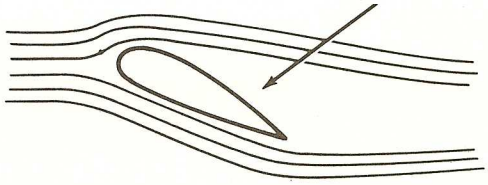

FIGURE 6 - TYPICAL FLOW REGIMES AND LIFT CHARACTERISTICS (REF. 3)

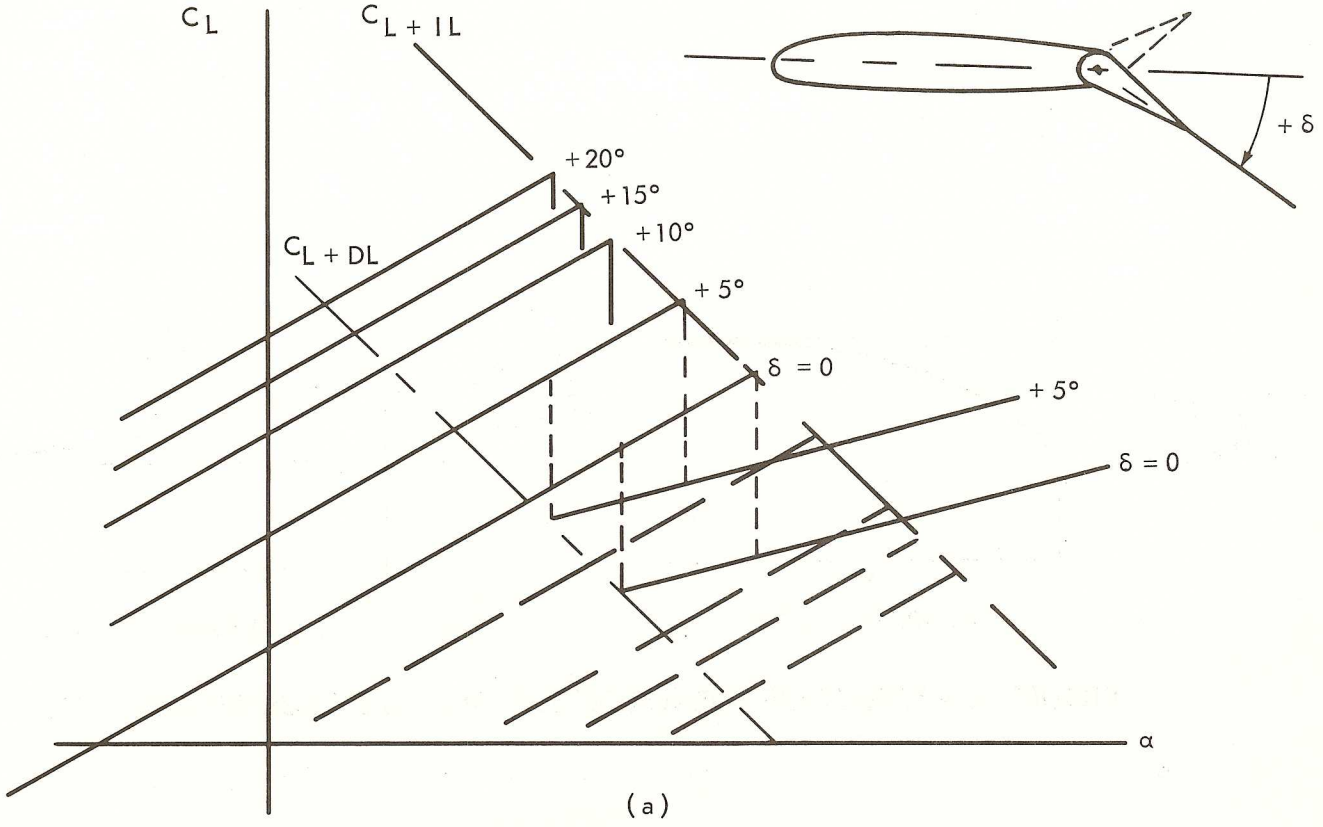

(a)

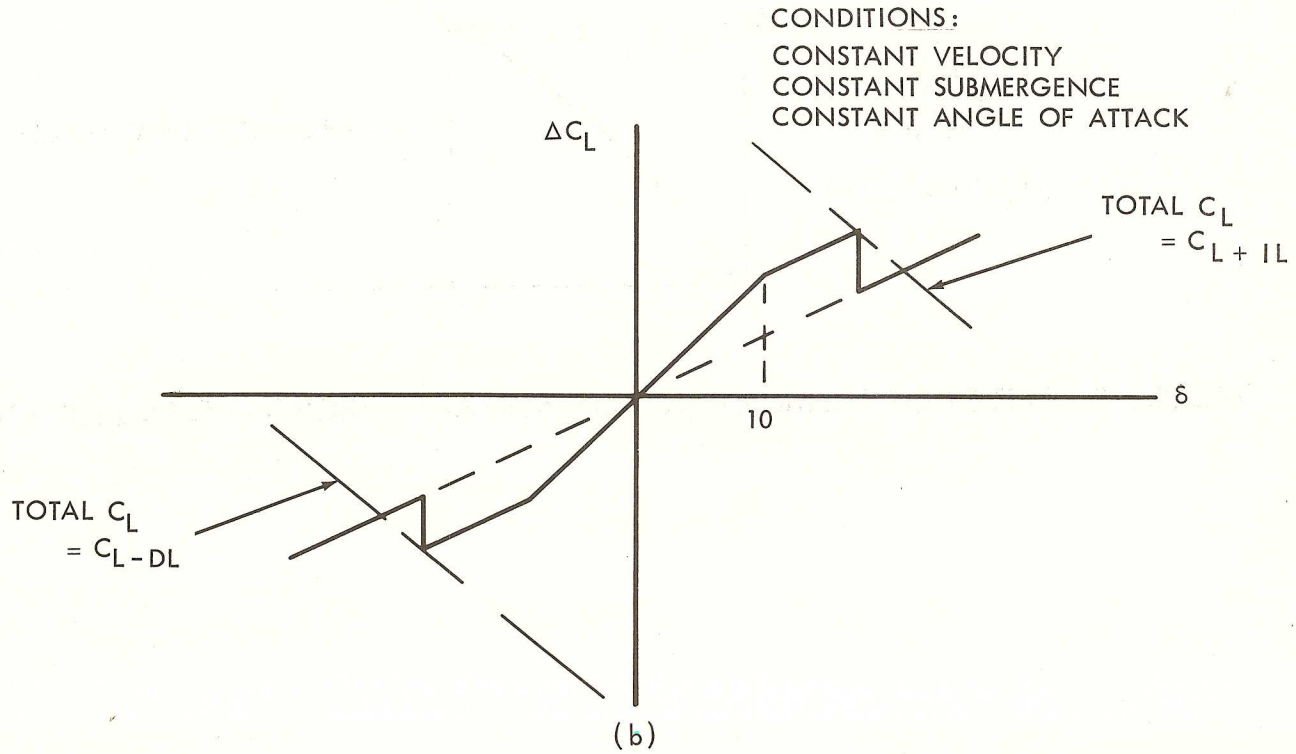

(b)

FIGURE 7 - EFFECTS OF FLAP DEFLECTION (REF. 3)

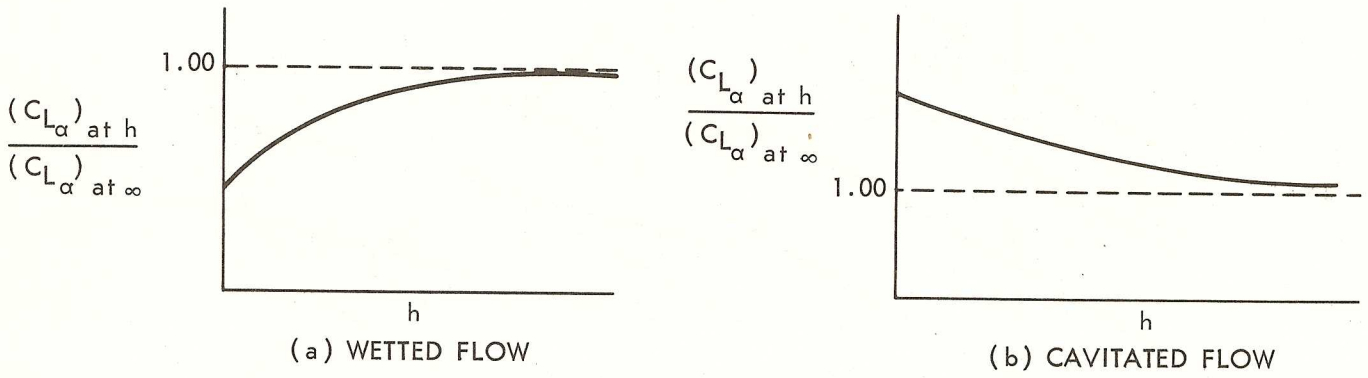

FIGURE 8 - EFFECT OF SUBMERGENCE ON FULLY SUBMERGED FOILS

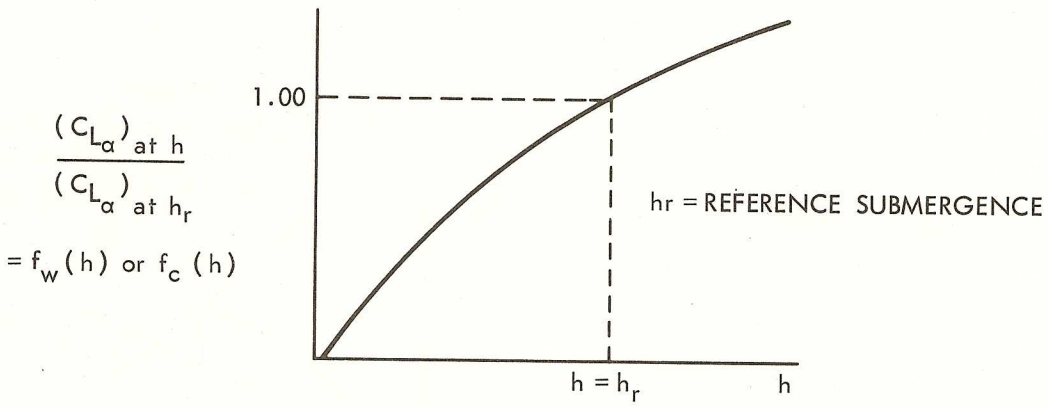

FIGURE 9 - EFFECT OF SUBMERGENCE ON SURFACE PIERCING FOILS AND STRUTS

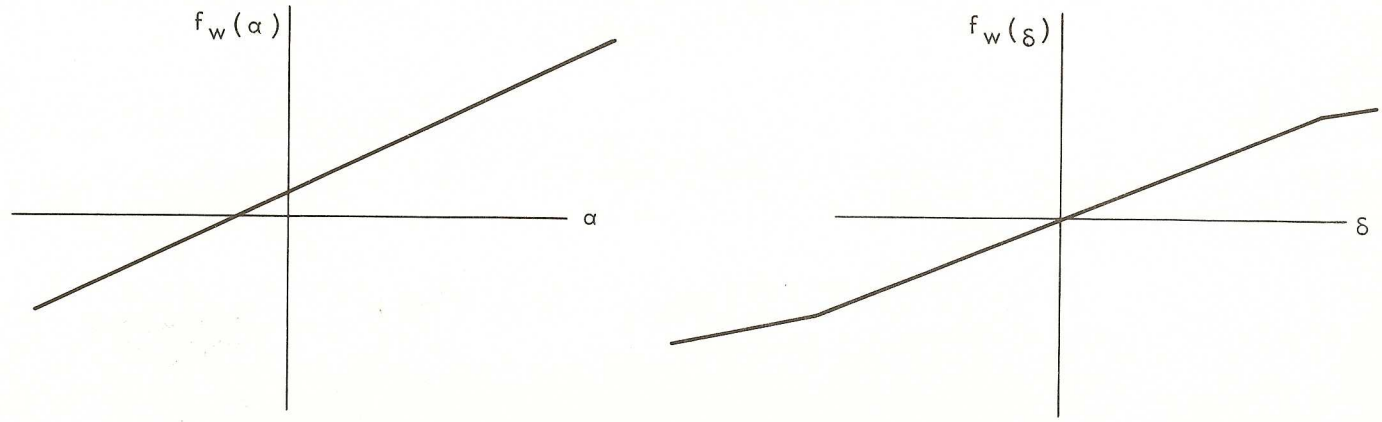

(a) FULLY WETTED FLOW

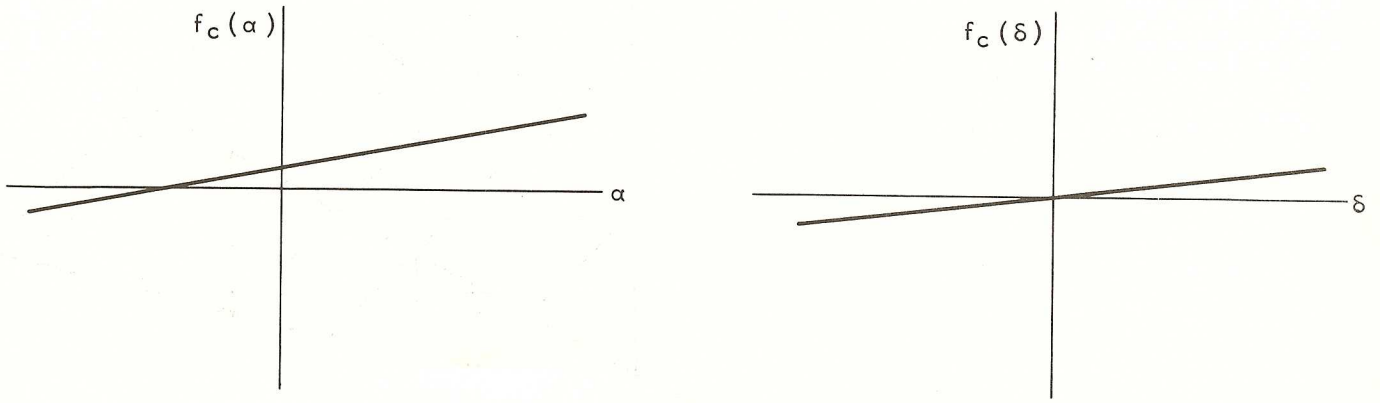

(b) FULLY CAVITATED FLOW

FIGURE 10 - FUNCTIONAL DEPENDENCE OF LIFT COEFFICIENT ON α AND δ AT REFERENCE DEPTH

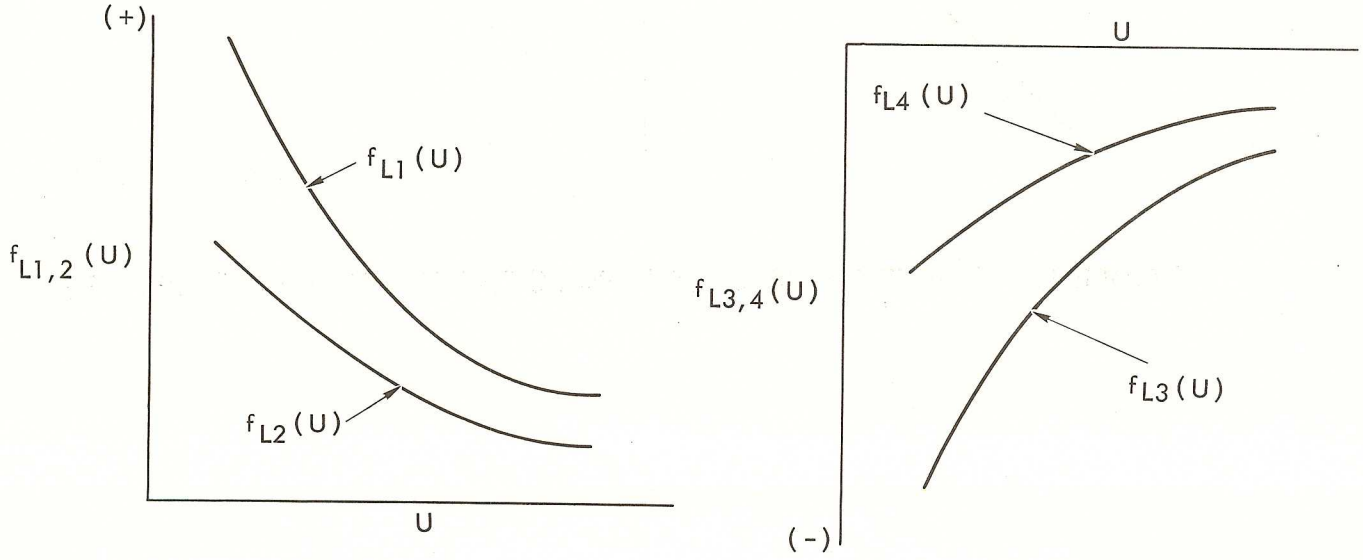

FIGURE 11 - FUNCTION OF VELOCITY AFFECTING LIFT

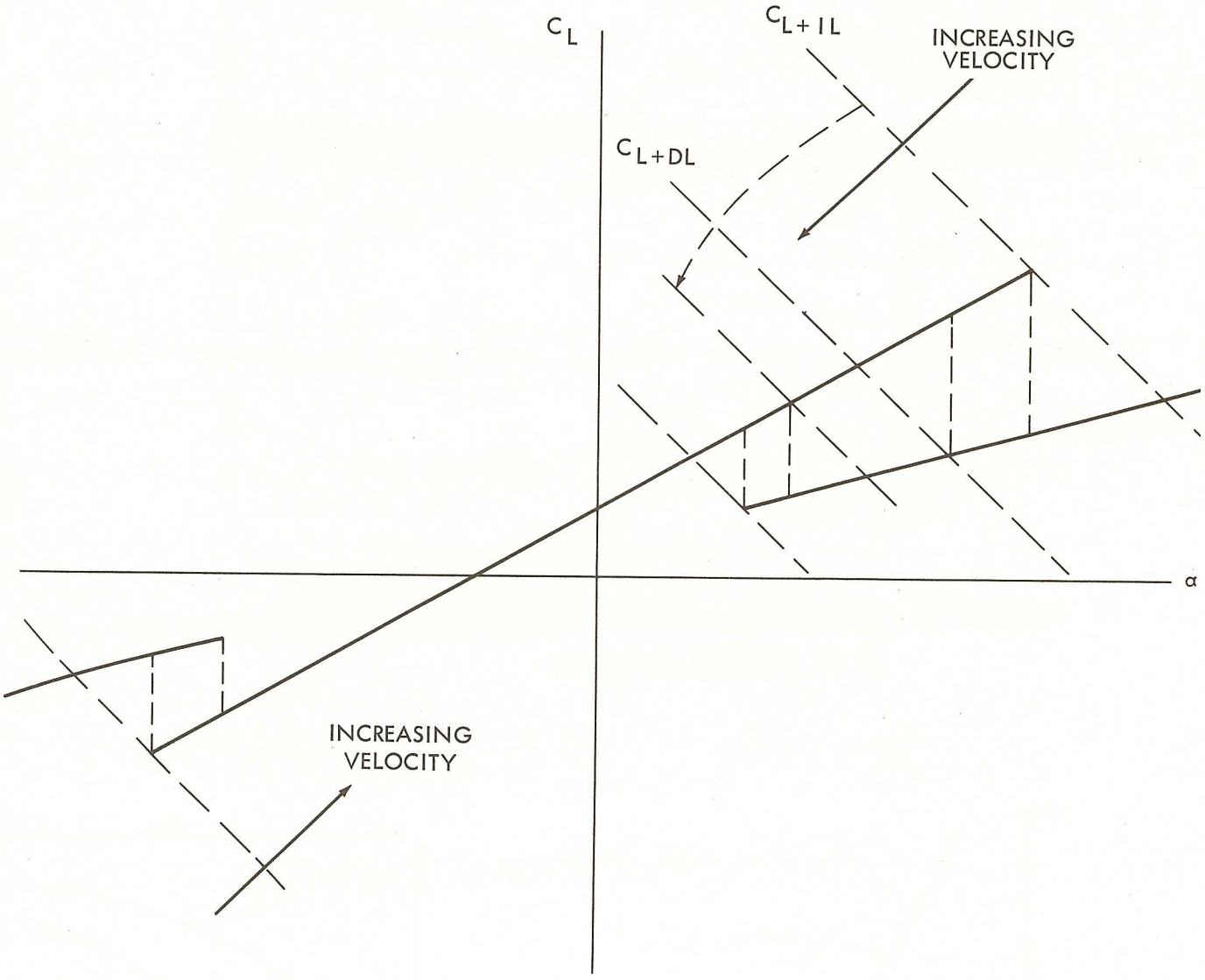

FIGURE 12 - EFFECT OF VELOCITY ON LOCATION OF LIMITS (REF. 3)

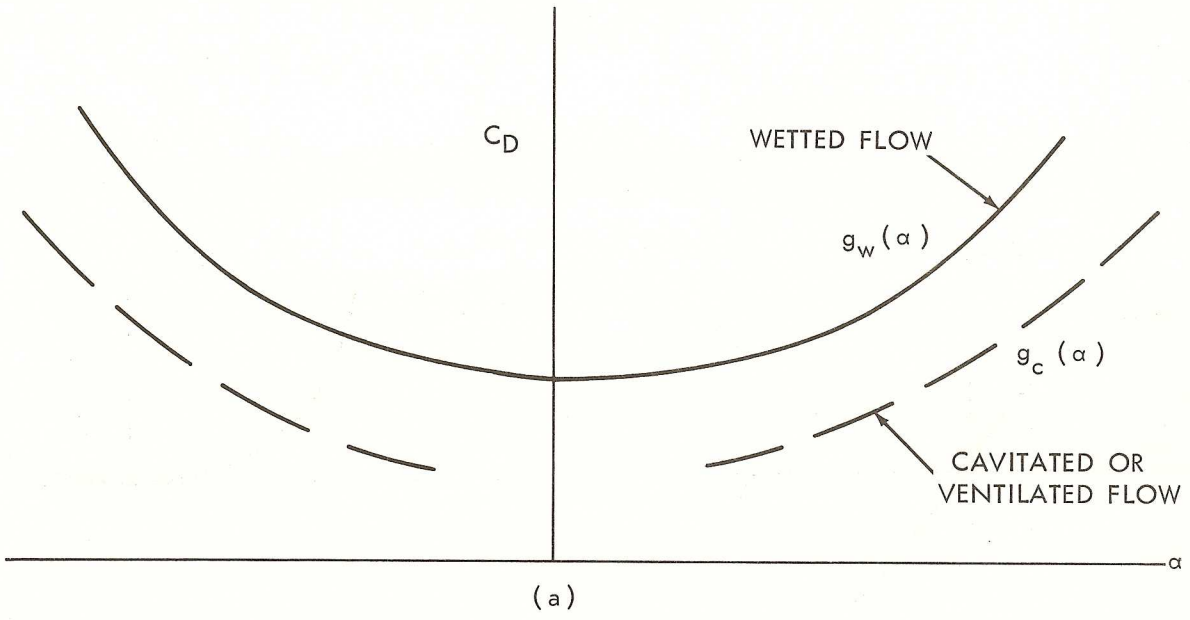

(a)

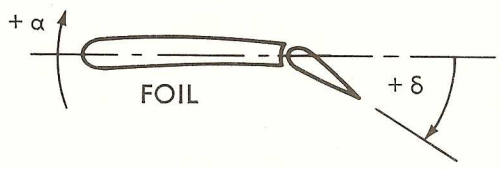

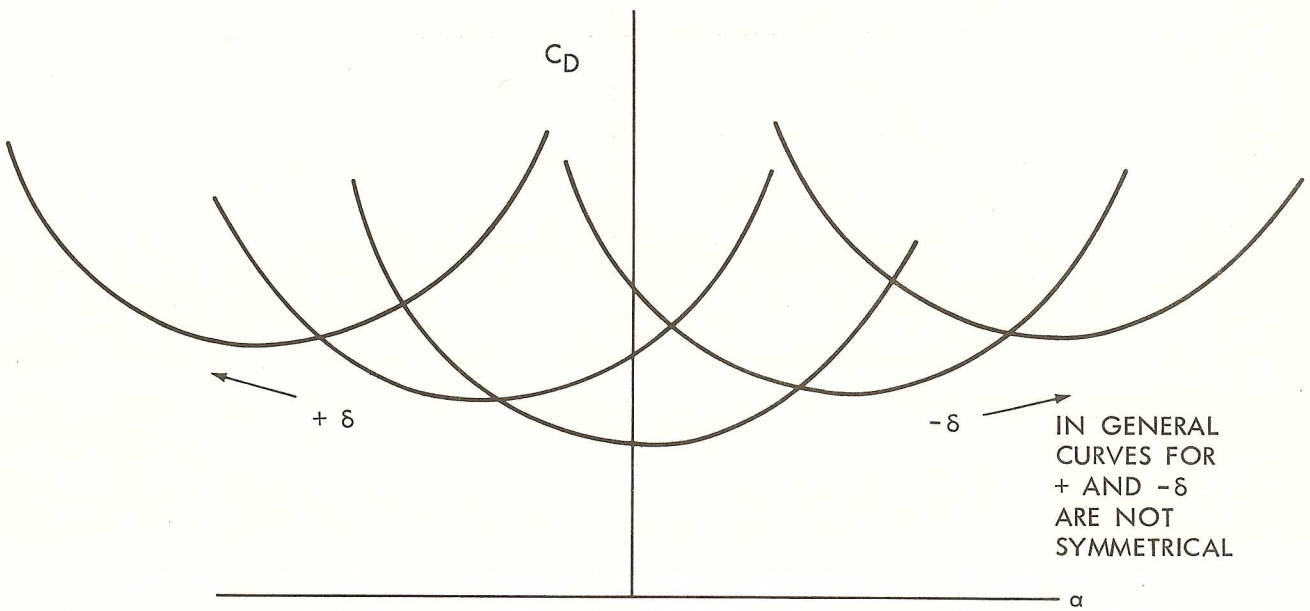

(b)

FIGURE 13 - BASIC DRAG COEFFICIENT CURVES

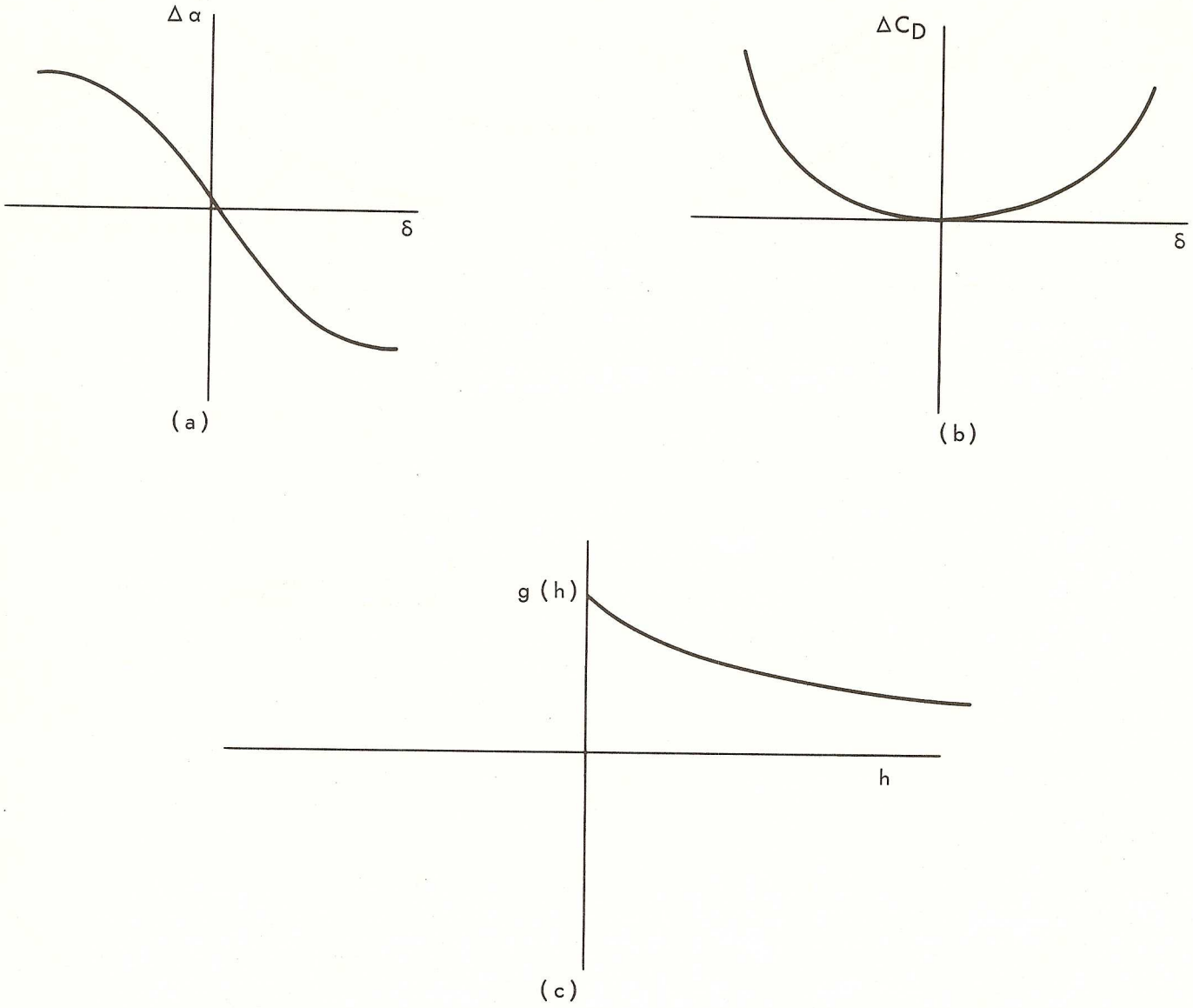

FIGURE 14 - FUNCTIONS FOR FOIL OR STRUT CONTROL SURFACE EFFECTS

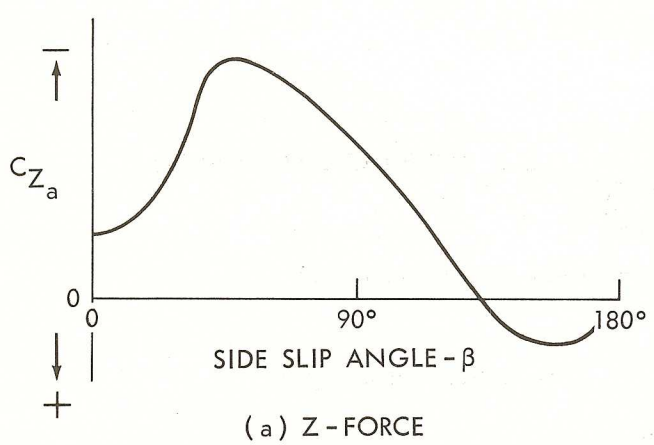

(a) Z - FORCE

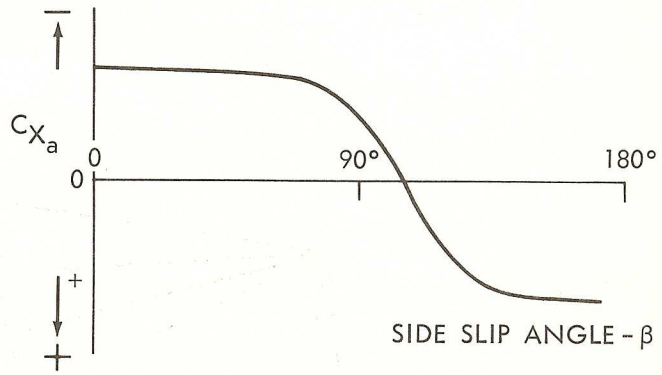

(b) X - FORCE

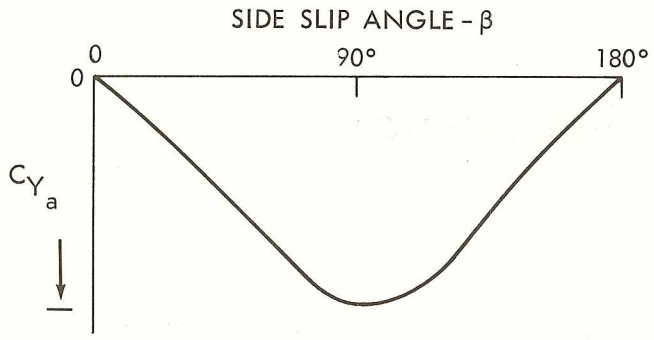

(c) Y - FORCE

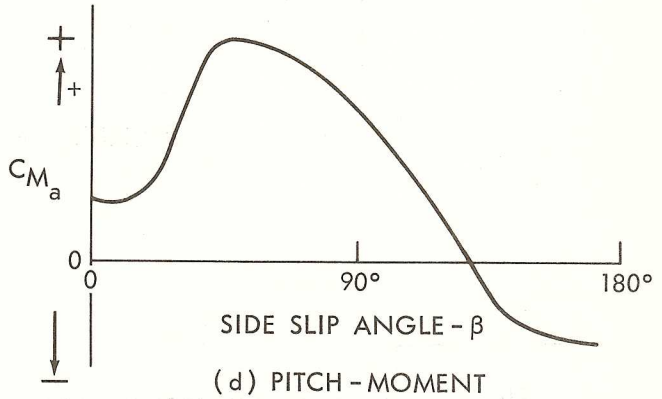

(d) PITCH - MOMENT

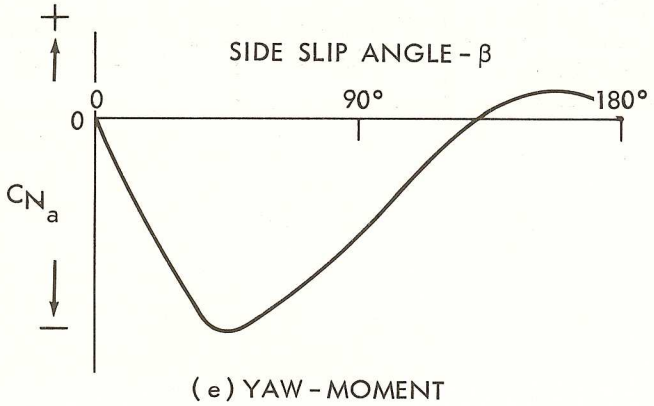

(e) YAW - MOMENT

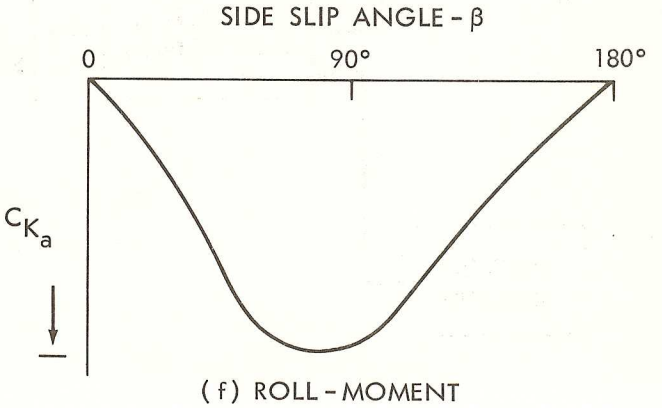

(f) ROLL - MOMENT

FIGURE 15 - TYPICAL AERODYNAMIC FORCE AND MOMENT COEFFICIENTS
θ = CONSTANT

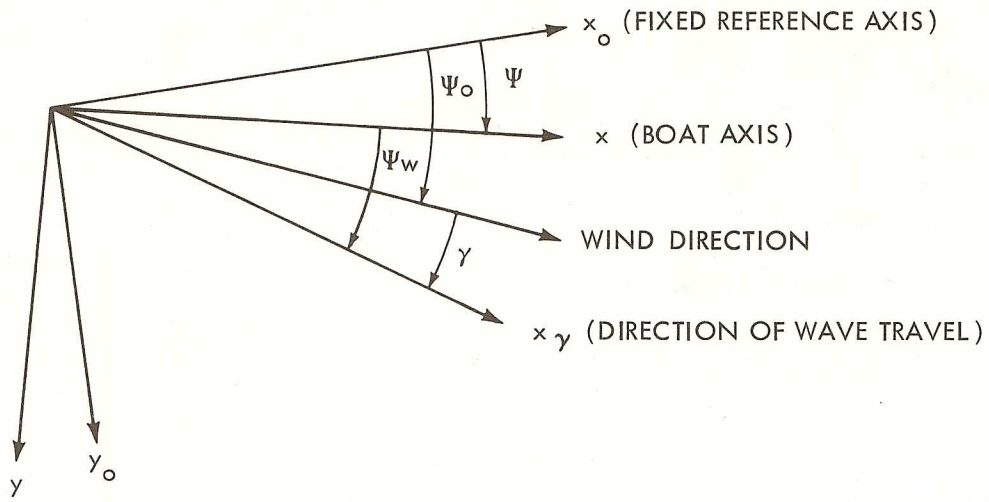

FIGURE 16 - DEFINITION SKETCH

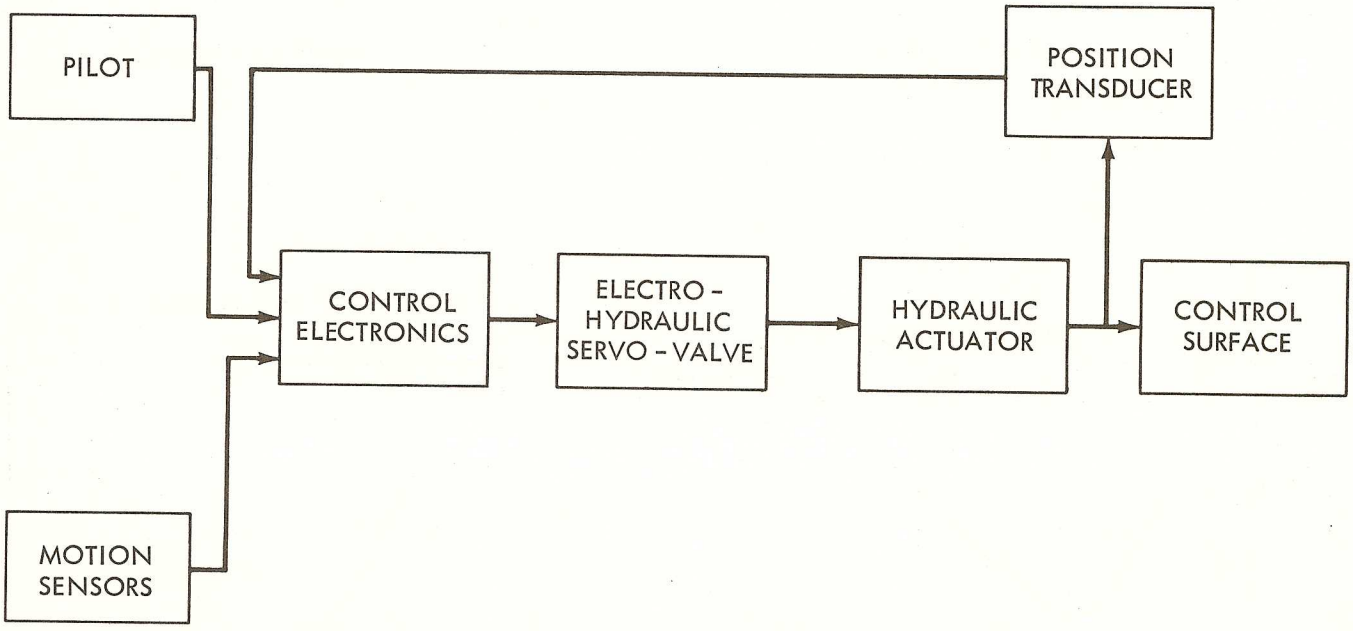

FIGURE 17 - TYPICAL CONTROL LOOP (REF. 3)

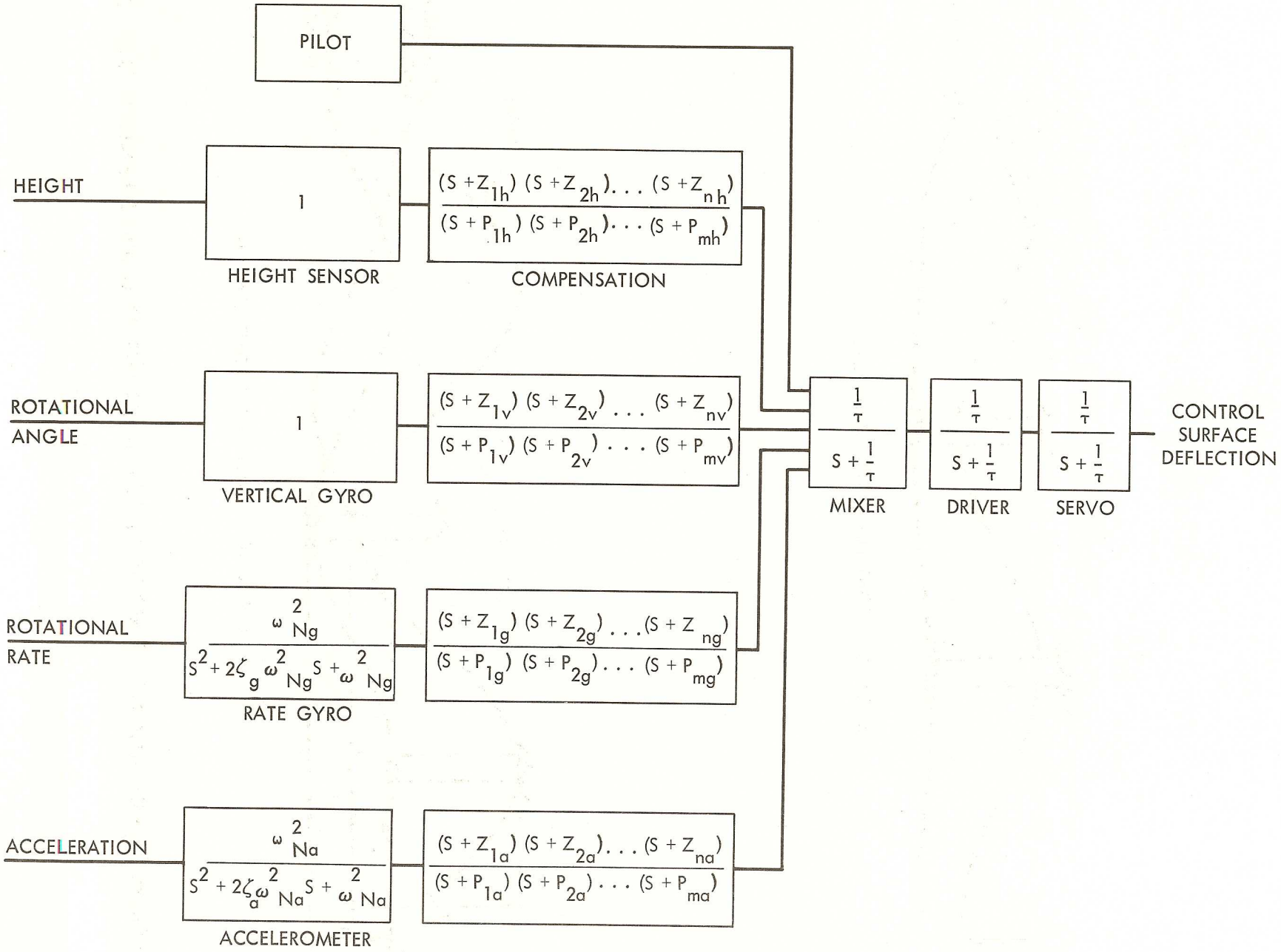

FIGURE 18 - EQUATIONS IN TYPICAL CONTROL CHANNEL (REF. 3)

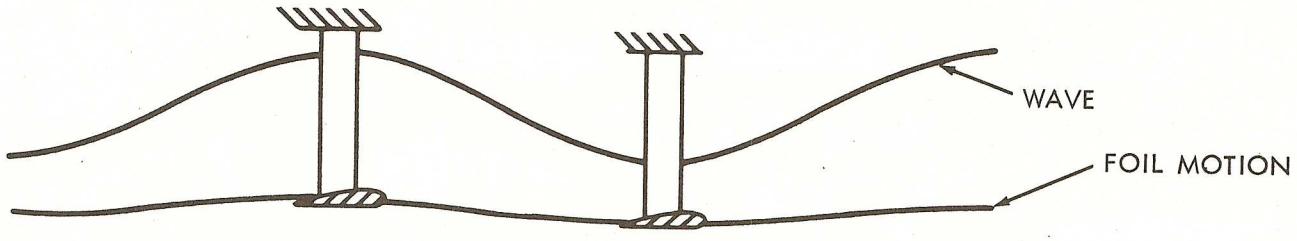

(a) WAVE HEIGHT LESS THAN STRUT LENGTH

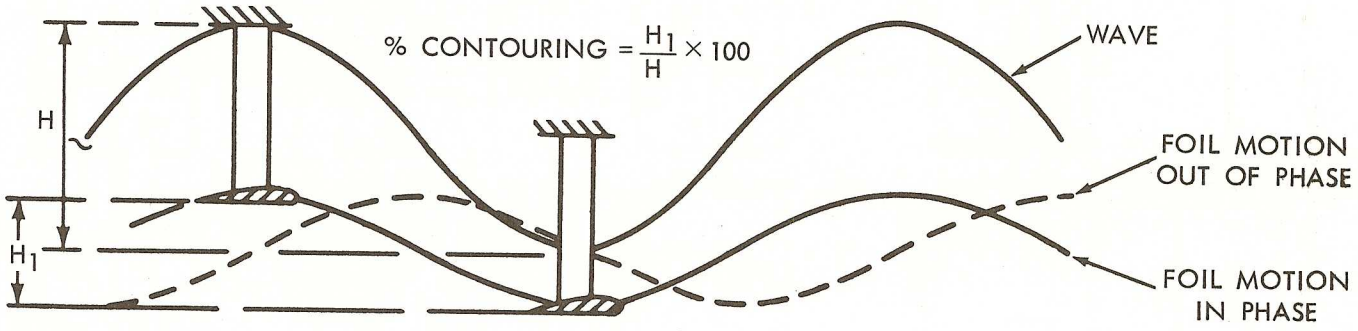

(b) WAVE HEIGHT GREATER THAN STRUT LENGTH

FIGURE 19 - RELATIONSHIP BETWEEN CONTOURING AND WAVE LENGTH (REF. 25)

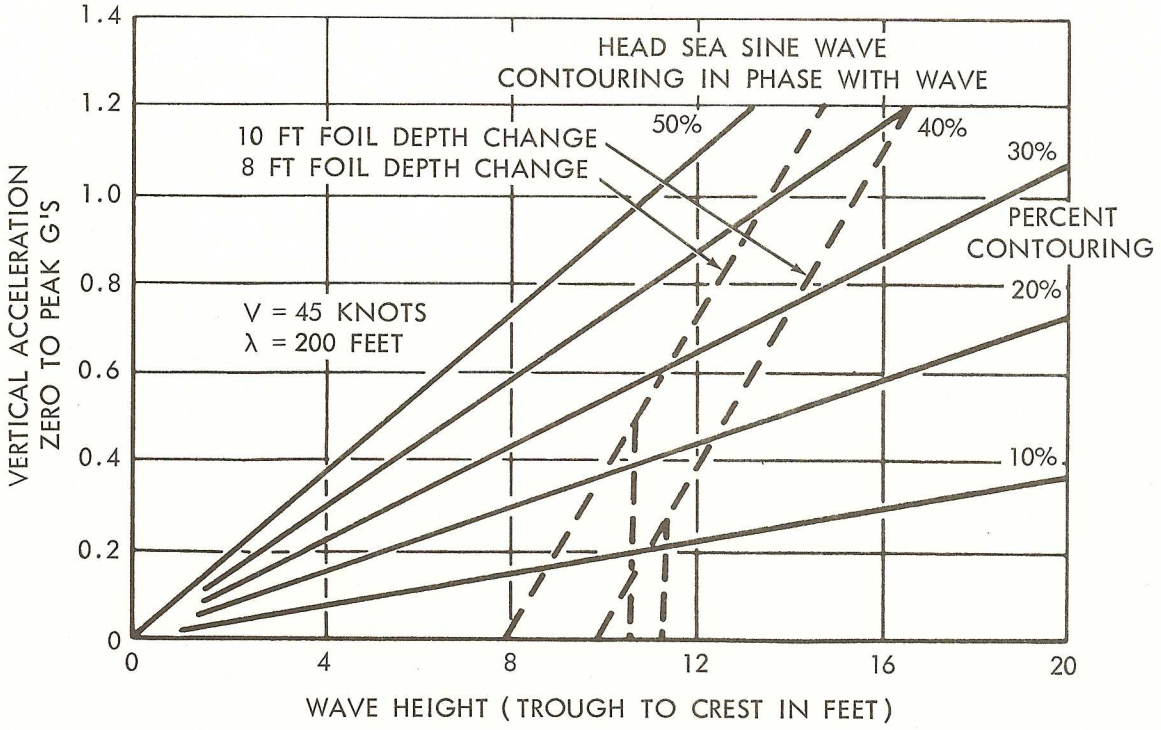

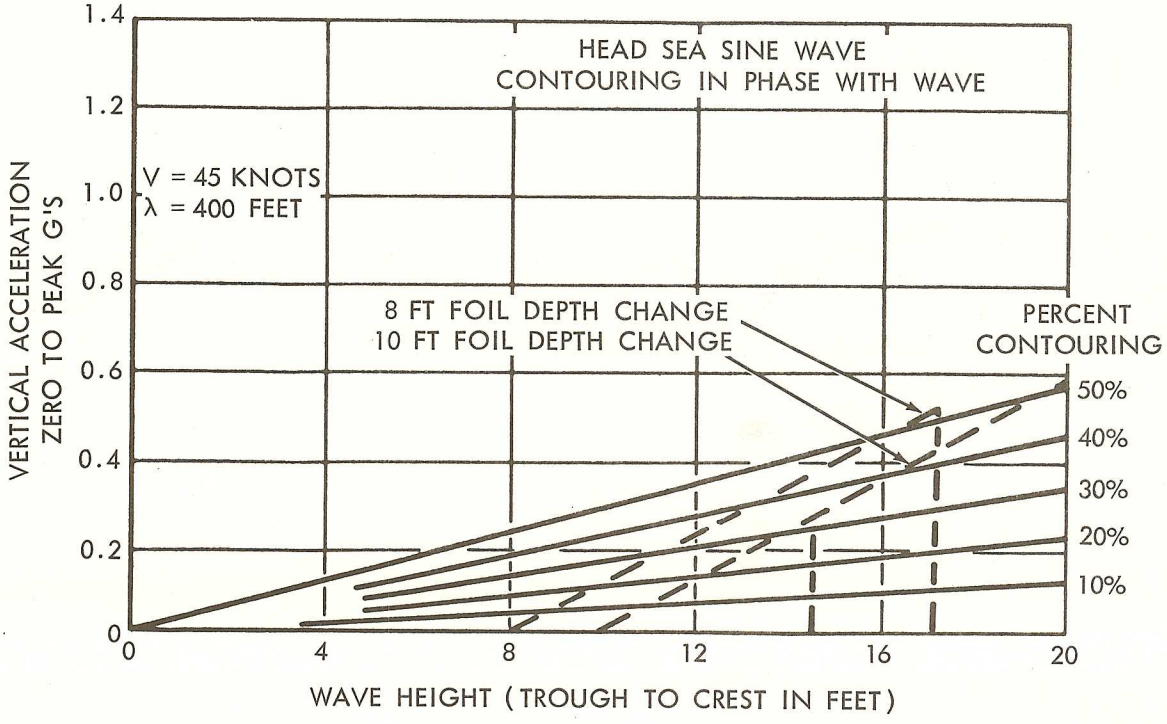

FIGURE 20 - RESULTANT G-LOADS VS WAVE HEIGHT AND PERCENT CONTOURING (REF. 25)

HYDRONAUTICS, Incorporated

DISTRIBUTION LIST
Contract No. NObs-90224

Chief, Naval Ship Systems Command
Department of the Navy
Washington 25, D. C. 20360
Attn: Code 210L 3
Code 345 1
Code 420 32
Code 442 1
Code 449 1
Code 632 1
Code 341B 1

Commanding Officer and Director
Naval Ship Research and
Development Center
Washington, D. C. 20007
Attn: Code 500 1
Code 513 1
Code 520 1
Code 526 1
Code 530 1
Code 580 1
Code 589 1
Code 142 2
Code 525 1

Naval Ship Research and
Development Center
High Speed Phenomena Division
Langley Field, Virginia
Attn: Mr. R. E. Olsen 1

Chief, Office of Naval Research
Department of the Navy
Washington 25, D. C.
Attn: Code 438 2

Aerojet General Corporation
Azusa, California
Attn: Mr. J. Levy 1

Chief, Bureau of Naval Weapons
Department of the Navy
Washington 25, D. C.
Attn: Code RAAD-334 1
Code RRSY-1 1

Mr. John B. Parkinson
Langley Aeronautical Laboratory
National Aeronautics and
Space Administration
Langley Air Force Base
Langley Field, Virginia 1

Chief of Naval Operations
Department of the Navy
Washington 25, D. C. 1

Scientific and Technical
Information Facility
Attn: NASA Representative
(SAK/DL-504)
P. O. Box 5700
Bethesda, Maryland 2

State University of Iowa
Iowa Institute of Hydraulic
Research,
Iowa City, Iowa 1

Southwest Research Institute
8500 Culebra Road
San Antonio 6, Texas
Attn: H. N. Abramson, Director
of Mech. Science 1

Defense Documentation Center
Cameron Station
Alexandria, Virginia 22314 20

Oceanics, Incorporated
Technical Industrial Park
Plainview, New York
Attn: Dr. Paul Kaplan 1

Stanford University
Stanford, California
Attn: Head, Civil Engr. 1

Boeing Airplane Company
Aero-Space Division
Box 3707
Seattle, Washington 1

California Inst. of Technology
Pasadean, California
Attn: Hydro Laboratory 1

Director, Stevens Institute
of Technology
Davidson Laboratory
Castle Point Station
Hoboken, New Jersey 1

HYDRONAUTICS, Incorporated
Pindell School Road
Howard County
Laurel, Maryland 1

Massachusetts Inst. of Technology
Dept. of Naval Architecture
and Marine Engineering
Cambridge 39, Massachusetts 1

St. Anthony Falls Hydraulic
Laboratory
University of Minnesota
Hennepin Island
Minneapolis 14, Minnesota 1

Technical Research Group, Inc.
Route 110, Melville, N. Y. 1

U. S. Navy Ordnance Test Station
Oceanic Research Group
3202 E. Foothill Blvd.
Pasadena, California 1

Lockheed Aircraft Corporation
Hydrodynamic Group
Sunnyvale, California
Attn: Mr. R. W. Kermeen 1

Grumman Aircraft Engr. Corp.
Marine Engr. Section
Bethpage, L.I. N. Y. 1

University of California
Inst. of Engr. Research
Berkeley, California
Attn: Prof. R. Paulling 1

General Dynamics/Convair
P. O. Box 1950
San Diego 12, California
Attn: Mr. R. Oversmith 1

U. S. Naval Training Devices
Center, Port Washington, N.Y.
Attn: Miss E. Colletti
Code 3322 1

Ordnance Research Laboratory
Post Office Box 30
State College, Penn. 16801
Attn: Prof. J.W. Holl 1

Commanding Officer and Director
U. S. Naval Electronic Lab.
San Diego 52, Calif. 92152
Attn: Library 1

UNCLASSIFIED

Security Classification

DOCUMENT CONTROL DATA - R&D

(Security classification of title, body of abstract and indexing annotation must be entered when the overall report is classified)

1. ORIGINATING ACTIVITY *(Corporate author)*
HYDRONAUTICS, Incorporated
Pindell School Road, Howard County,
Laurel, Maryland 20810

2a. REPORT SECURITY CLASSIFICATION
Unclassified

2b. GROUP

3. REPORT TITLE
HYDROFOIL CRAFT DYNAMICS IN A REALISTIC SEA INCLUDING AUTOMATIC CONTROL

4. DESCRIPTIVE NOTES *(Type of report and inclusive dates)*
Technical Report

5. AUTHOR(S) *(Last name, first name, initial)*
M. Martin

6. REPORT DATE	7a. TOTAL NO. OF PAGES	7b. NO. OF REFS
November 1967	87	42

8a. CONTRACT OR GRANT NO.
NObs-90224 and N00014-67-C-0417

b. PROJECT NO. SS600-000, Task 1701

c.

d.

9a. ORIGINATOR'S REPORT NUMBER(S)
T. R. 463-10

9b. OTHER REPORT NO(S) *(Any other numbers that may be assigned this report)*

10. AVAILABILITY/LIMITATION NOTICES
Distribution of this document is unlimited.

11. SUPPLEMENTARY NOTES

12. SPONSORING MILITARY ACTIVITY
Naval Ship Systems Command
Department of the Navy

13. ABSTRACT

The six degrees of freedom equations of motion of a hydrofoil boat in short crested seas are presented. An attempt has been made to make these equations as realistic as feasible by taking into account the more important non-linearities, such as the variations in the wetted area and hydrodynamic coefficients of the struts and surface piercing hydrofoils with submergence changes, changes in hydrodynamic forces and moments resulting from cavitation and ventilation, etc. Equations representing the seaway and the control system are also presented and discussed. Feedback control considerations leading to desirable stability and motions in waves are discussed.

DD FORM 1 JAN 64 1473

D23558

UNCLASSIFIED

Security Classification

14. KEY WORDS	LINK A		LINK B		LINK C	
	ROLE	WT	ROLE	WT	ROLE	WT
Hydrofoil Boat Motions Simulation Equations of Motion Seaway Craft Force Dynamics						

INSTRUCTIONS

1. ORIGINATING ACTIVITY: Enter the name and address of the contractor, subcontractor, grantee, Department of Defense activity or other organization *(corporate author)* issuing the report.

2a. REPORT SECURITY CLASSIFICATION: Enter the overall security classification of the report. Indicate whether "Restricted Data" is included. Marking is to be in accordance with appropriate security regulations.

2b. GROUP: Automatic downgrading is specified in DoD Directive 5200.10 and Armed Forces Industrial Manual. Enter the group number. Also, when applicable, show that optional markings have been used for Group 3 and Group 4 as authorized.

3. REPORT TITLE: Enter the complete report title in all capital letters. Titles in all cases should be unclassified. If a meaningful title cannot be selected without classification, show title classification in all capitals in parenthesis immediately following the title.

4. DESCRIPTIVE NOTES: If appropriate, enter the type of report, e.g., interim, progress, summary, annual, or final. Give the inclusive dates when a specific reporting period is covered.

5. AUTHOR(S): Enter the name(s) of author(s) as shown on or in the report. Enter last name, first name, middle initial. If military, show rank and branch of service. The name of the principal author is an absolute minimum requirement.

6. REPORT DATE: Enter the date of the report as day, month, year; or month, year. If more than one date appears on the report, use date of publication.

7a. TOTAL NUMBER OF PAGES: The total page count should follow normal pagination procedures, i.e., enter the number of pages containing information.

7b. NUMBER OF REFERENCES: Enter the total number of references cited in the report.

8a. CONTRACT OR GRANT NUMBER: If appropriate, enter the applicable number of the contract or grant under which the report was written.

8b, 8c, & 8d. PROJECT NUMBER: Enter the appropriate military department identification, such as project number, subproject number, system numbers, task number, etc.

9a. ORIGINATOR'S REPORT NUMBER(S): Enter the official report number by which the document will be identified and controlled by the originating activity. This number must be unique to this report.

9b. OTHER REPORT NUMBER(S): If the report has been assigned any other report numbers *(either by the originator or by the sponsor)*, also enter this number(s).

10. AVAILABILITY/LIMITATION NOTICES: Enter any limitations on further dissemination of the report, other than those imposed by security classification, using standard statements such as:

(1) "Qualified requesters may obtain copies of this report from DDC."

(2) "Foreign announcement and dissemination of this report by DDC is not authorized."

(3) "U. S. Government agencies may obtain copies of this report directly from DDC. Other qualified DDC users shall request through _____."

(4) "U. S. military agencies may obtain copies of this report directly from DDC. Other qualified users shall request through _____."

(5) "All distribution of this report is controlled. Qualified DDC users shall request through _____."

If the report has been furnished to the Office of Technical Services, Department of Commerce, for sale to the public, indicate this fact and enter the price, if known.

11. SUPPLEMENTARY NOTES: Use for additional explanatory notes.

12. SPONSORING MILITARY ACTIVITY: Enter the name of the departmental project office or laboratory sponsoring *(paying for)* the research and development. Include address.

13. ABSTRACT: Enter an abstract giving a brief and factual summary of the document indicative of the report, even though it may also appear elsewhere in the body of the technical report. If additional space is required, a continuation sheet shall be attached.

It is highly desirable that the abstract of classified reports be unclassified. Each paragraph of the abstract shall end with an indication of the military security classification of the information in the paragraph, represented as *(TS), (S), (C), or (U)*.

There is no limitation on the length of the abstract. However, the suggested length is from 150 to 225 words.

14. KEY WORDS: Key words are technically meaningful terms or short phrases that characterize a report and may be used as index entries for cataloging the report. Key words must be selected so that no security classification is required. Identifiers, such as equipment model designation, trade name, military project code name, geographic location, may be used as key words but will be followed by an indication of technical context. The assignment of links, rules, and weights is optional.